NACA

RESEARCH MEMORANDUM

for the

Air Materiel Command, U. S. Air Force

INVESTIGATION OF THE EFFECT OF TIP TANKS ON THE WING LOADING OF A REPUBLIC F-84 AIRPLANE IN THE AMES 40- BY 80-FOOT WIND TUNNEL

By Lynn W. Hunton, Joseph K. Dew, and Ralph D. Salisbury

Ames Aeronautical Laboratory
Moffett Field, Calif.

NATIONAL ADVISORY COMMITTEE
FOR AERONAUTICS

WASHINGTON

Feb. 2, 1949

NATIONAL ADVISORY COMMITTEE FOR AERONAUTICS

RESEARCH MEMORANDUM

for the

Air Materiel Command, U. S. Air Force

INVESTIGATION OF THE EFFECT OF TIP TANKS ON THE WING LOADING OF A REPUBLIC F-84 AIRPLANE IN THE AMES 40- BY 80-FOOT WIND TUNNEL

By Lynn W. Hunton, Joseph K. Dew, and Ralph D. Salisbury

SUMMARY

Wind-tunnel tests at low Mach number of a Republic F-84C airplane were conducted to determine by pressure-distribution measurements the air loads on wing-tip tanks and the change in wing load distribution due to the presence of tip tanks. Measurements of the aeroelastic twist of the wing were also obtained.

Results are presented in the form of loading coefficient, center-of-pressure location, pitching-moment coefficient, aerodynamic-center location, and aeroelastic twist. The investigation revealed that the redistributions in loading brought about by either the tip tanks or elastic deformation of the wing were relatively small when compared with the changes in loading normally associated with the deflection of an aileron.

INTRODUCTION

The Republic F-84 airplane is a high-performance jet-propelled fighter employing many of the latest ideas regarding high-speed airplanes. However, with the adoption of jettisonable wing-tip fuel tanks (hereafter referred to as tanks), there began a series of accidents involving wing-structure failures of various forms ranging from mere skin wrinkling to complete shearing of a wing panel. Generally, the accidents were restricted to flight conditions of high Mach number (0.8 approximately) at low altitude (below 10,000

ft). Since the installation of the tank was the only change made, it appeared that in some manner the tank on the tip of the wing was causing a redistribution in wing loading. Such a change in wing loading could conceivably lead to a condition of aeroelastic divergence of the wing resulting in wing failures. Since the character of such a redistribution in loading, exclusive of compressibility effects, could be determined at low speed, the Air Force requested that tests of an F-84C airplane be conducted in the Ames 40- by 80-foot wind tunnel. Furthermore, such a full-scale test on the actual flight article afforded an opportunity to determine, insofar as possible, the aeroelastic characteristics of the wing.

It was proposed to include in the investigation measurements of the distribution of pressure over the right wing and tank and the aeroelastic twist of the wing. The investigation was to cover (1) configuration changes involving the tank, wing-tip-to-tank gap seal, and aileron deflection; (2) the full range of test airspeeds attainable in the tunnel; and (3) an angle-of-attack range limited to the lower angles as dictated by the high-speed flight conditions under which trouble was occurring. The results of the investigation, presented herein in the form of summary plots, were obtained through integrations of the faired pressure-distribution-data curves. The great mass of pressure-distribution data have been omitted from this report.

SYMBOLS

Symbols used in the present report are defined as follows:

$\frac{c_{n_w} c}{c_{av}}$ section loading coefficient of the wing

$\frac{c_{n_t} d}{d_{av}}$ section loading coefficient of the tank

c_{n_w} section normal-force coefficient of the wing $\left(\frac{\text{local normal force}}{qc}\right)$

c_{n_t} section normal-force coefficient of the tank $\left(\frac{\text{local normal force}}{qd}\right)$

C_{N_t} tank normal-force coefficient $\left(\frac{\text{total normal force}}{qS_t}\right)$

c_{m_w} wing section pitching-moment coefficient about quarter chord $\left(\frac{\text{pitching moment}}{qc\bar{c}}\right)$

C_{m_t} tank pitching-moment coefficient about half-chord line of wing $\left(\frac{\text{pitching moment}}{qS_t l}\right)$

b wing span, 36.42 feet

c local wing chord, feet

c_{av} average wing chord $\left(\frac{S}{b}\right)$, 7.13 feet

$\bar{c}$ mean aerodynamic chord $\left(\frac{\int_0^{b/2} c^2 dy}{\int_0^{b/2} c\, dy}\right)$, 7.40 feet

d local tank diameter, feet

d_{av} average tank diameter $\left(\frac{S_t}{l}\right)$, 1.58 feet

l tank length, 12.65 feet

q free-stream dynamic pressure, pounds per square foot

S wing area, 260 square feet

S_t tank area projected on a horizontal plane through the axis of symmetry, 20 square feet

V free-stream velocity, miles per hour

x longitudinal coordinate measured either from wing leading edge or tank nose parallel to plane of symmetry, feet

$\frac{y}{b/2}$ dimensionless lateral coordinate of wing

y lateral coordinate measured from wing root perpendicular to the plane of symmetry, feet

α angle of attack of fuselage thrust axis, degrees

β angle of sideslip (positive for right wing forward), degrees

δ_a aileron deflection, degrees

θ angle of aeroelastic twist, degrees

DESCRIPTION OF THE APPARATUS

The Republic F-84C airplane is a jet-propelled fighter characterized by conventional straight wings and a nose inlet. A three-view drawing showing the pertinent dimensions of the airplane is given in figure 1. The wings had an aspect ratio of 5.1, a tip-to-root-chord ratio of 0.56, and a uniform twist giving 2° of washout at the tips. The theoretical section of the wing (see table I for ordinates) was constant over the span, was cambered for a lift coefficient of 0.15 with the maximum thickness of 12 percent located at the 0.45-chord point, and had a 17° trailing-edge angle. Landing flaps on the wing were single slotted while the ailerons were an internally-sealed pressure-balance type. The tips of the wings were designed to accommodate jettisonable fuel tanks as shown in figure 2(a). Figure 2(b) shows the installation of the wood and clay fairing used to seal the gap between the wing tip and tank.

For the load-distribution measurements the right-wing panel and tank were instrumented with flush-type pressure orifices. The wing contained 200 orifices located at 5 spanwise stations while the tank was equipped with 260 orifices located in rings at 22 lengthwise stations. Details of the wing and tank station locations are given in figure 3. Photographing of the several banks of manometer boards provided the means of recording the pressure data.

For purposes of the investigation of aeroelastic characteristics of the wing, it was necessary to support the airplane with a special cradle-type structure which had no attachments to the airplane outboard of the wing-root pin connection. Supported in this manner, as shown in the photographs of the test setup arrangement of figure 4, the wing was allowed to undergo distortion in a normal free-flight manner with the exception of mass inertia effects. Instrumentation for this phase of the investigation consisted of a 35 millinterfocal plane shutter camera mounted in the right side of the fuselage near the 0.50-chord line station of the wing and about 10 inches above the wing upper surface. Reference lines on the wing and tank were painted at several constant percent-chord and span locations. In addition, a grid was fixed in the camera in contact with the film to provide a fixed reference index on each exposure.

TESTS

The investigation included two types of tests: pressure-distribution measurements over the wing and tank, and measurements of the aeroelastic twist of the wing. For the pressure measurements, tests were made of the airplane (1) in the clean condition, (2) with the right tank installed, (3) with the right tank and a 10° up-deflection of the right aileron, (4) with the right aileron deflected up 10°, and (5) with the right tank installed and the wing-tip-to-tank gap faired and sealed. These tests were made at several angles of attack and angles of sideslip of the airplane at a test airspeed of 126 miles per hour. This airspeed corresponds to a Reynolds number of about 8.7×10^6 based on the mean aerodynamic chord of 7.4 feet. In addition, for some of the airplane configurations, pressure tests were made at an angle of attack of 2.2° for test airspeeds of 179 and 233 miles per hour.

To determine the elastic qualities of the wing in twist, tests were made of the airplane both in the clean condition and with the tank installed for angles of attack of the airplane of 2.2°, 4.3°, and 8.5° and for airspeeds ranging from 88 to 240 miles per hour.

Corrections for air-stream inclination and tunnel boundary effects have been applied to all angle-of-attack data throughout the report.

RESULTS AND DISCUSSION

Loading Characteristics

Pressure-distribution data were obtained over the tank and wing for the various configurations of the airplane involving combinations of the tank, tank fairing, and aileron as given in the outline of results in table II. Integration of the section pressure-distribution plots of these data gave the load-distribution characteristics for the wing and the tip tank as shown in figures 5 to 9 and 10 and 11, respectively.

For the wing, these results include the spanwise variation of the section loading coefficient and the section center-of-pressure location. The former are presented for several angles of attack, angles of sideslip, and test airspeeds, while the latter are presented only for several angles of attack and sideslip. Throughout these results no attempt has been made to estimate the wing loading characteristics inboard of station 1 (0.35 semispan). Likewise,

the results for the configurations involving the tank installation have been terminated at station 5 located at 96 percent of the semi-span. In the tests of the wing with the tank in the faired condition, the fairing seal covered a majority of the outboard wing-section orifices which thus accounts for the omission of these tip-station data throughout the results for this configuration. In figure 5(d), the portion of data omitted for 2.2° in angle of attack was not obtained due to the faulty operation of one of the pressure recording cameras.

From an inspection of these load-distribution characteristics for the wing, it may be seen that (1) the installation of the tank causes no appreciable change in the wing loading and causes a reduction in the effectiveness of the aileron; (2) the installation of the tank fairing increases the loading over the wing uniformly by an amount equivalent to a lift coefficient of about 0.04; (3) 5° of sideslip of the wing with or without tanks causes no significant change in the wing load distribution; and (4) an increase in the test airspeed resulted in a general rise in the measured loadings over the wing which, from the distribution of the increment, would appear to be attributable to some form of angle-of-attack change. (A check of possible wing deformation or deflection of the tunnel support system revealed no explanation for the results.)

The integrated results for the tank (figs. 10 and 11) include the lengthwise variation of the section loading coefficient both for several angles of attack and several test airspeeds. In figures 10(b) and 11(b), it may be noted that the loading curves over the aft portion of the tank for angles of attack 2.2° and 8.5° are represented by dashed lines. Owing to camera recording trouble, this part of the data was missed but has been estimated from other similar test results. The foregoing load-distribution diagrams for the tank were integrated to obtain summary curves of the total normal-force coefficient, center-of-pressure location, and pitching-moment coefficient. These results, as a function of angle of attack of the airplane, are presented in figures 12 to 14 for each of the three tank configurations tested. Of significant note from these tank results are (1) the increase in the tank normal-force coefficient (fig. 12) caused by sealing the wing-tip-to-tank gap and (2) the influence of the wing pressures on the tank loading as evidenced by the decrease in tank normal-force coefficient caused by the negative deflection of the aileron.

Figures 15(a) to 15(d) have been prepared in order to show directly the effect of the tank installation on the spanwise-loading

coefficient, center-of-pressure location, pitching-moment coefficient, and aerodynamic-center location, respectively, of the wing. These comparisons are shown for an angle of attack of the airplane of 2.2° which corresponds to an acceleration of approximately 4g based on a flight speed of 0.8 Mach number, an altitude of 5000 feet, and small-scale force tests. (See reference 1.) With the exception of the aerodynamic-center comparison, the fairing of the curves for the wing-tank combination have been extended past the wing tip to a point on the outboard side of the tank equivalent to the mean diameter of the tank. Thus, a general indication of the over-all loading on the wing is shown based on the tank-pressure-distribution data, but computed in terms of the dimensions of the projected wing tip at the center line of the tank. An inspection of these comparisons reveals only small alterations in the wing loading characteristics which may be considered negligible in comparison with the changes in loading caused by a deflection of the aileron. Similar comparisons at the higher angles of attack reveal equally negligible effects of the tank on the wing. Therefore, based on the results of these low-speed pressure-distribution tests it may be concluded that, barring compressibility effects, the wing failure accidents experienced by F-84 airplanes with tip tanks cannot be attributed to wing divergence as the result of a redistribution in wing loading induced by the presence of the tank on the wing tip.

Aeroelastic Characteristics

The method of measuring the aeroelastic twist of the wing is illustrated in figure 16 by a few representative samples of the twist measurement photographs. The samples show the twist data for the wing, with and without the tank, obtained at test dynamic pressures of 0 and 100 pounds per square foot and angles of attack of the airplane of 2.2°, 4.3°, and 8.5°. For example, the degree of twist over the wing span was obtained from this figure by comparing the attitude of corresponding sections of the wing as measured at the two test dynamic pressures of 0 and 100 pounds per square foot.

The results of the aeroelastic twist investigation, made at test dynamic pressures ranging from 20 to 140 pounds per square foot, are presented in figures 17(a) and 17(b) for the wing in the clean condition and with the tank installed, respectively. For both of these configurations, values of the twist as a function of test dynamic pressure are shown for angles of attack of 2.2°, 4.3°, and 8.5° and at semispan locations of 0.4, 0.6, and 0.8. Also included in figure 17(b) are data showing the twist of the tank itself relative

to the fuselage reference line. Over the relatively limited airspeed range covered in this low-speed investigation, the results show the twist to be a linear function of the dynamic pressure. By comparing the data obtained for the wing with and without tank, it may be seen that for a given semispan location and angle of attack the tank caused only a slight increment in wing twist. For an angle of attack of 2.2°, which attitude in flight represents the aerodynamic loading for a 4g acceleration at high speed, computations made of the wing-section-load changes and center-of-pressure movement due to the twist indicated negligible changes even for the values of twist measured at the top tunnel speed. Since detailed information on the characteristics of the wing structure was not available, no attempt was made to interpret these twist results in terms of wing-divergence characteristics for the airplane at high-flight speed. However, if the trend found in these low-speed tests of a linear variation of twist with flight dynamic pressure extends over the full-flight-speed range, then it would appear that changes in the wing characteristics would assume serious enough proportions to warrant further investigation at high-flight speed.

Ames Aeronautical Laboratory,
National Advisory Committee for Aeronautics,
Moffett Field, Calif.

REFERENCES

1. Gillis, Clarence L., and Andrews, Thomas B., Jr.: Wind-Tunnel Tests of a 1/5-Scale Model of the Republic XP-84 Airplane. Part I - Longitudinal Static Stability and Control. NACA MR No. L6D05, 1946.

TABLE I.- WING AIRFOIL ORDINATES

Station x/c in percent chord	Ordinates in percent chord	
	Upper	Lower
0.50	0.947	0.808
.75	1.193	1.005
1.25	1.538	1.283
2.50	2.161	1.793
5.00	3.023	2.488
7.50	3.678	2.962
10	4.212	3.337
15	5.022	3.923
20	5.625	4.345
25	6.108	4.630
30	6.465	4.845
35	6.712	4.983
40	6.855	5.063
45	6.918	5.078
50	6.884	5.020
55	6.738	4.875
60	6.463	4.633
65	6.037	4.272
70	5.492	3.785
75	4.794	3.203
80	3.970	2.543
85	3.028	1.847
90	2.027	1.152
95	.990	.540
100	0	0

L.E. radius height = 0.055 percent chord
L.E. radius = 0.800 percent chord

TABLE II.- INDEX TO THE FIGURES OF BASIC PRESSURE-DISTRIBUTION RESULTS

Results	Configuration	Variable	Fig. No.
Wing			
Spanwise loading	Wing	α	5(a)
Do.	Wing + tank	α	(b)
Do.	Wing + tank + $\delta_a{}^{-10}$	α	(c)
Do.	Wing + $\delta_a{}^{-10}$	α	(d)
Do.	Wing + tank faired	α	(e)
Spanwise loading	Wing	β,α	6(a)
Do.	Wing + tank	β,α	(b)
Do.	Wing + tank + $\delta_a{}^{-10}$	β,α	(c)
Spanwise loading	Wing	V	7(a)
Do.	Wing + tank	V	(b)
Do.	Wing + tank + $\delta_a{}^{-10}$	V	(c)
Spanwise center of pressure	Wing	α	8(a)
Do.	Wing + tank	α	(b)
Do.	Wing + tank + $\delta_a{}^{-10}$	α	(c)
Do.	Wing + $\delta_a{}^{-10}$	α	(d)
Do.	Wing + tank faired	α	(e)
Spanwise center of pressure	Wing	β,α	9(a)
Do.	Wing + tank	β,α	(b)
Do.	Wing + tank + $\delta_a{}^{-10}$	β,α	(c)
Tank			
Lengthwise loading	Wing + tank	α	10(a)
Do.	Wing + tank + $\delta_a{}^{-10}$	α	(b)
Do.	Wing + tank faired	α	(c)
Lengthwise loading	Wing + tank	V	11(a)
Do.	Wing + tank + $\delta_a{}^{-10}$	V	(b)

FIGURE LEGENDS

Figure 1.– Three-view drawing of the Republic F-84 airplane with tip tanks.

Figure 2.– Views of the fuel tank installation on the tip of the wing.

Figure 3.– Location of the pressure orifice stations on the Republic F-84 airplane wing and tip tank.

Figure 4.– Views of the test installation of the Republic F-84C airplane in the Ames 40- by 80-foot wind tunnel. (a) Front view.

Figure 4.– Concluded. (b) Three-quarter front view.

Figure 5.– Spanwise loading on the wing for several angles of attack. Test airspeed, 126 mph; β,0°. (a) Clean wing.

Figure 5.– Continued. (b) Tip tank on.

Figure 5.– Continued. (c) Tip tank on, aileron angle -10°.

Figure 5.– Continued. (d) Aileron angle -10°.

Figure 5.– Concluded. (e) Tip tank on, wing-tip-to-tank gap sealed.

Figure 6.– Effect of sideslip on the spanwise loading of the wing at several angles of attack. Test airspeed, 126 mph. (a) Clean wing.

Figure 6.– Continued. (b) Tip tank on.

Figure 6.– Concluded. (c) Tip tank on, aileron angle -10°.

Figure 7.– Spanwise loading on the wing for several test airspeeds. α, 2.2°; β,0°. (a) Clean wing.

Figure 7.– Continued. (b) Tip tank on.

Figure 7.– Concluded. (c) Tip tank on, aileron angle -10°.

Figure 8.– Spanwise center-of-pressure location on the wing for several angles of attack. Test airspeed, 126 mph; β,0°. (a) Clean wing.

Figure 8.– Continued. (b) Tip tank on.

Figure 8.– Continued. (c) Tip tank on, aileron angle -10°.

Figure 8.– Continued. (d) Aileron angle -10°.

Figure 8.– Concluded. (e) Tip tank on, wing–tip–to–tank gap sealed.

Figure 9.– Effect of sideslip on the spanwise center–of–pressure location on the wing at several angles of attack. Test airspeed, 126 mph. (a) Clean wing.

Figure 9.– Continued. (b) Tip tank on.

Figure 9.– Concluded. (c) Tip tank on, aileron angle -10°.

Figure 10.– Tank load distribution for several angles of attack. Test airspeed, 126 mph; $\beta,0^{\circ}$. (a) Plain tank.

Figure 10.– Continued. (b) Aileron angle -10°.

Figure 10.– Concluded. (c) Wing–to–tank gap sealed.

Figure 11.– Tank load distribution for several test airspeeds. α, 2.2°; $\beta,0^{\circ}$. (a) Plain tank.

Figure 11.– Concluded. (b) Aileron angle -10°.

Figure 12.– Variation of tank normal–force coefficient with angle of attack as affected by several configuration changes. Test airspeed, 126 mph; $\beta,0^{\circ}$.

Figure 13.– Variation of tank center–of–pressure location with angle of attack as affected by several configuration changes. Test airspeed, 126 mph; $\beta,0^{\circ}$.

Figure 14.– Variation of tank pitching–moment coefficient with angle of attack as affected by several configuration changes. Test airspeed, 126 mph; $\beta,0^{\circ}$.

Figure 15.– Comparisons of the spanwise characteristics of the wing with and without the tip tank. Test airspeed, 126 mph; α, 2.2°. (a) Section loading coefficient.

Figure 15.– Continued. (b) Section center–of–pressure location.

Figure 15.– Continued. (c) Section pitching-moment coefficient.

Figure 15.– Concluded. (d) Section aerodynamic-center location.

Figure 16.– Sample aeroelastic twist measurement photographs of the wing with and without the tip tank. β,0°. (a) α, 2.2°.

Figure 16.– Continued. (b) α, 4.3°.

Figure 16.– Concluded. (c) α, 8.5°.

Figure 17.– Variation of the aeroelastic twist of the wing with test dynamic pressure for several semispan stations and angles of attack. β,0°. (a) Clean wing.

Figure 17.– Concluded. (b) Tip tank on.

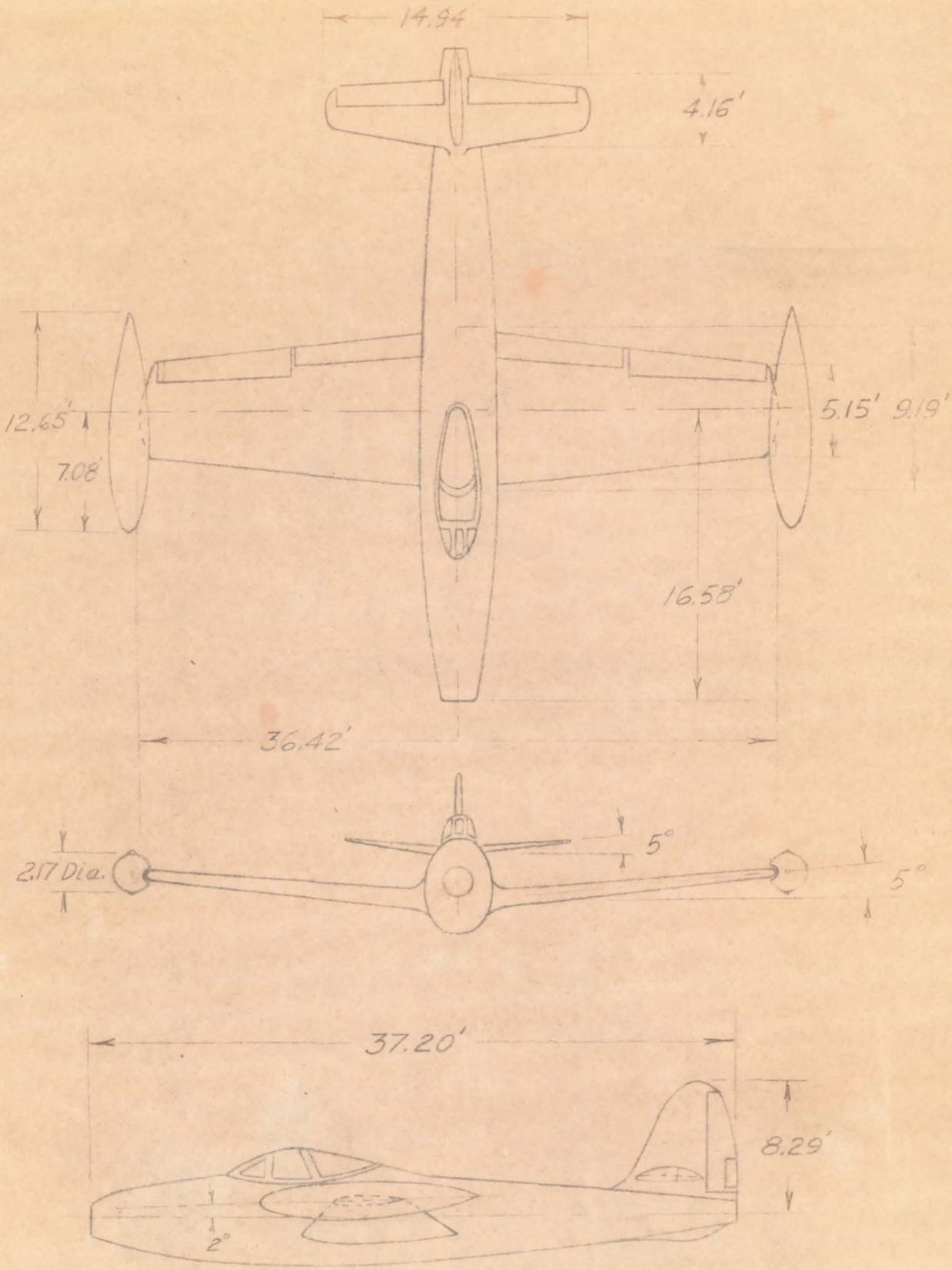

Figure 1.— Three-view drawing of the Republic F-84 airplane with tip tanks.

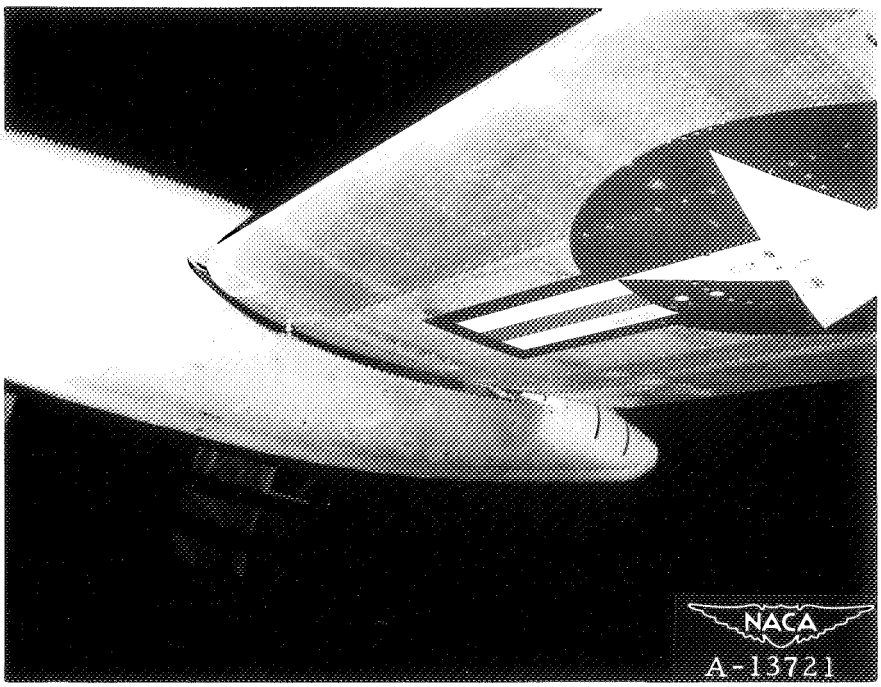

(a) Wing-to-tank gap unsealed.

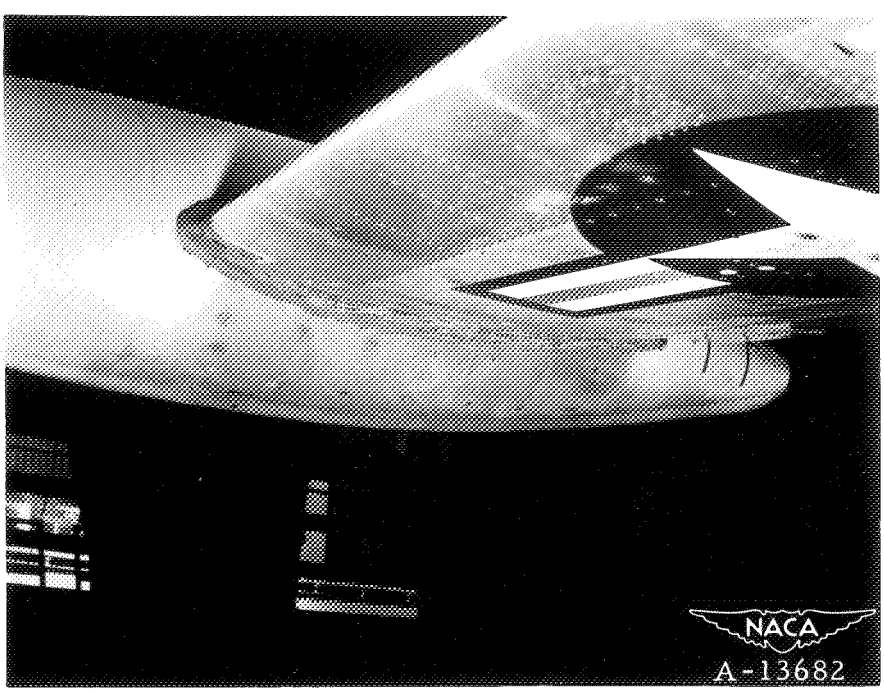

(b) Wing-to-tank gap faired and sealed.

Figure 2.- Views of the fuel tank installation on the tip of the wing.

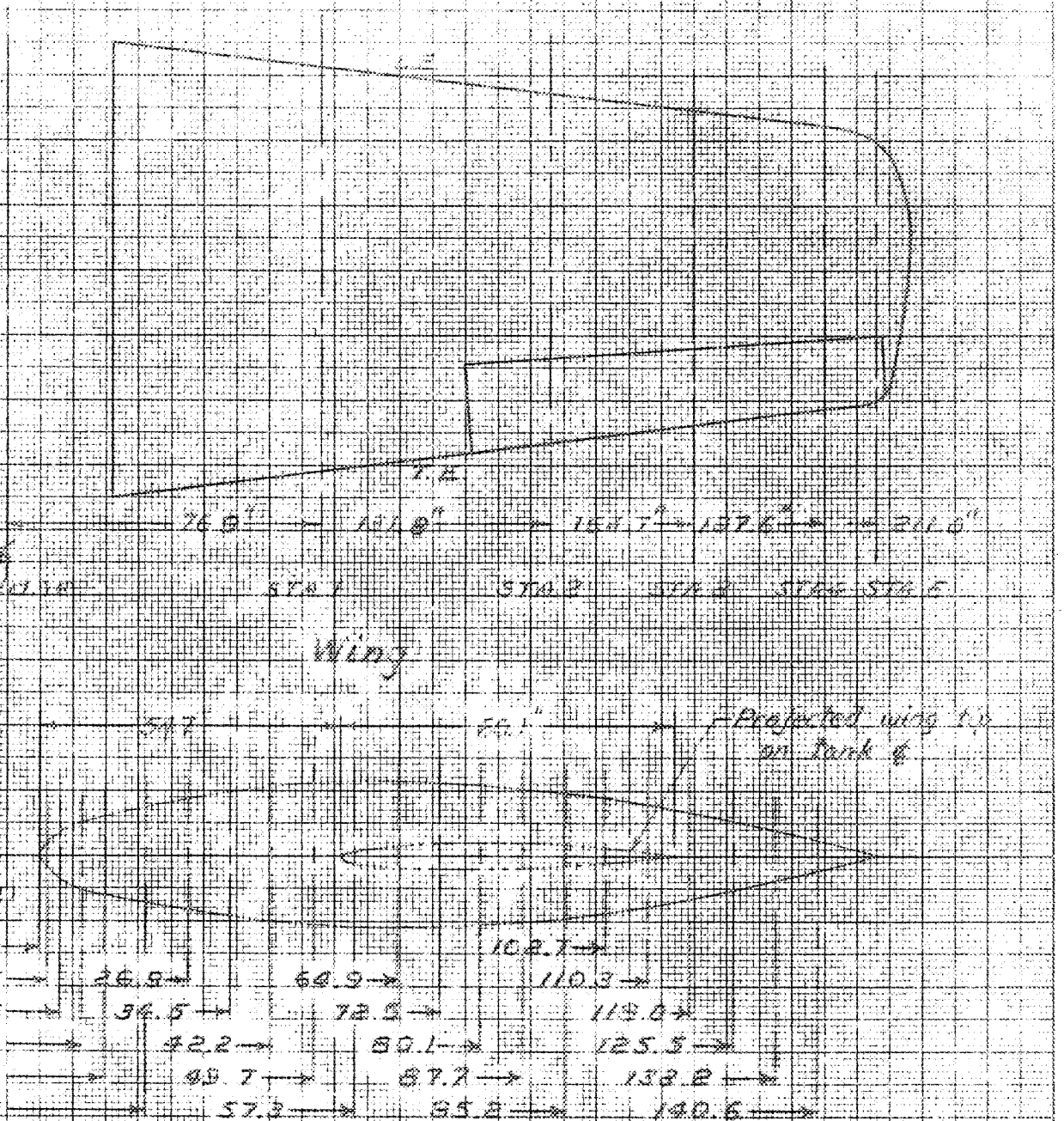

Figure 3. - Location of the pressure orifices on the wing and wing tip tank.

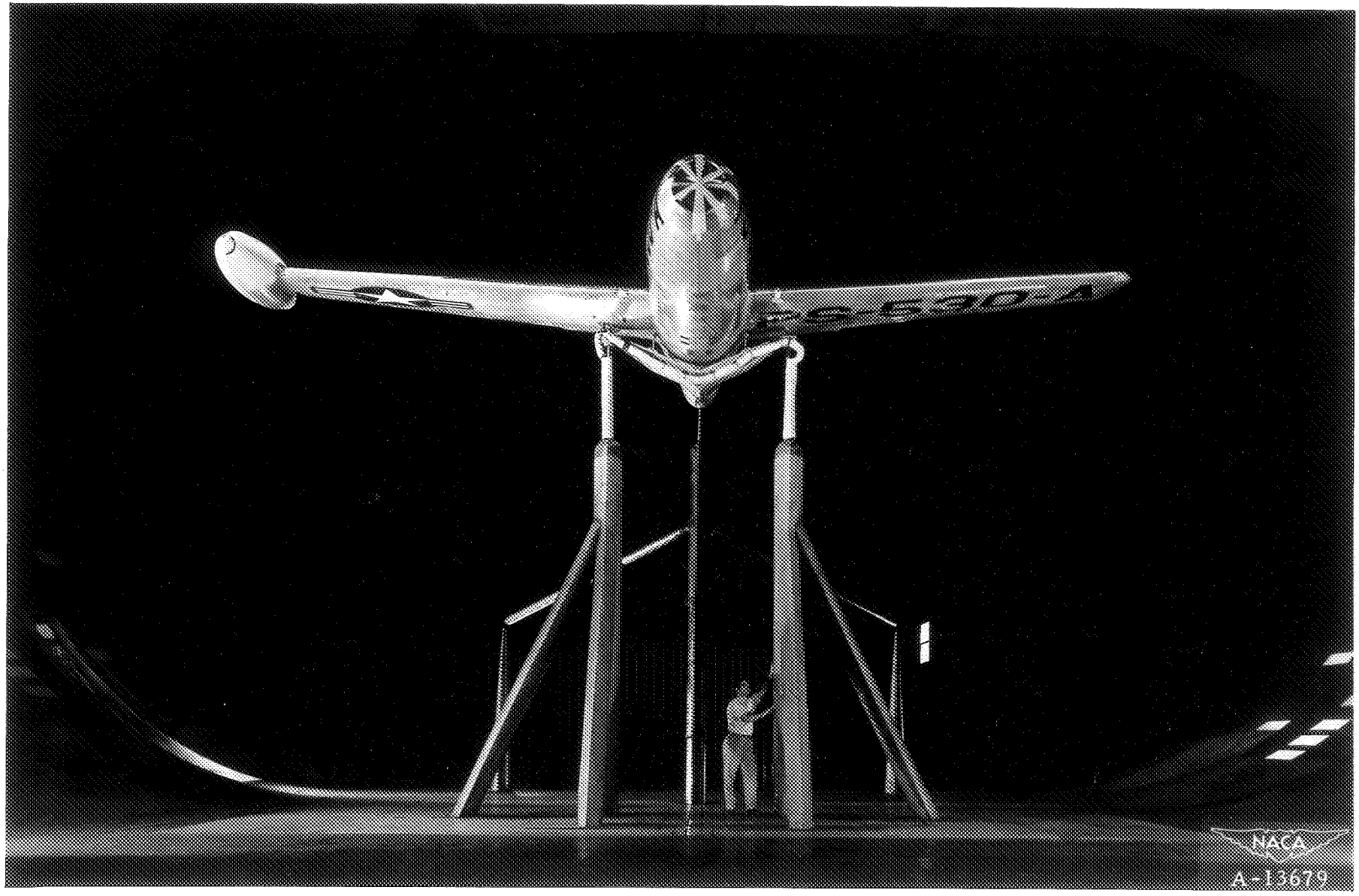

(a) Front view.

Figure 4.- Views of the test installation of the Republic F-84C airplane in the Ames 40- by 80-foot wind tunnel.

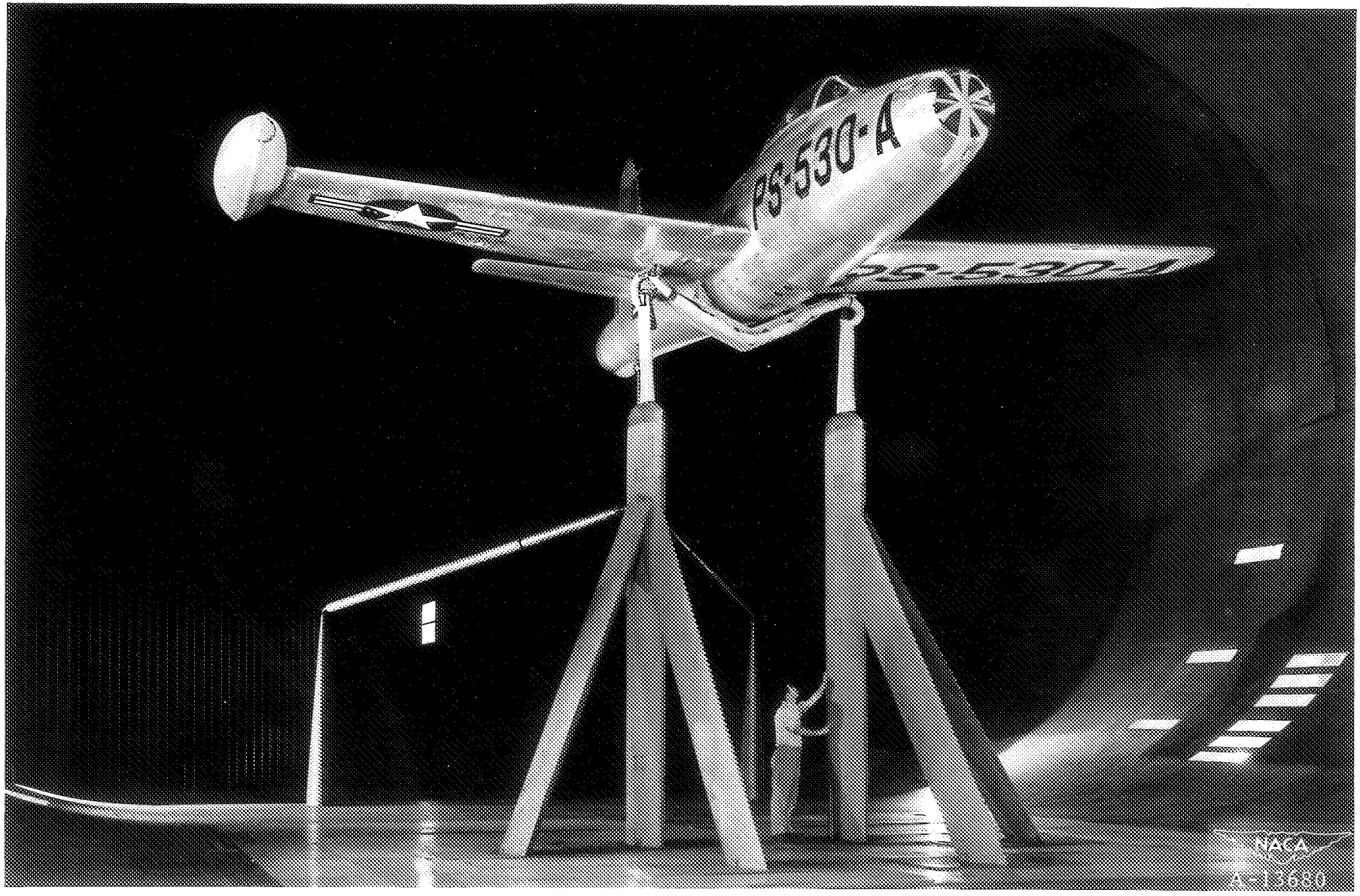

(b) Three-quarter front view.

Figure 4.- Concluded.

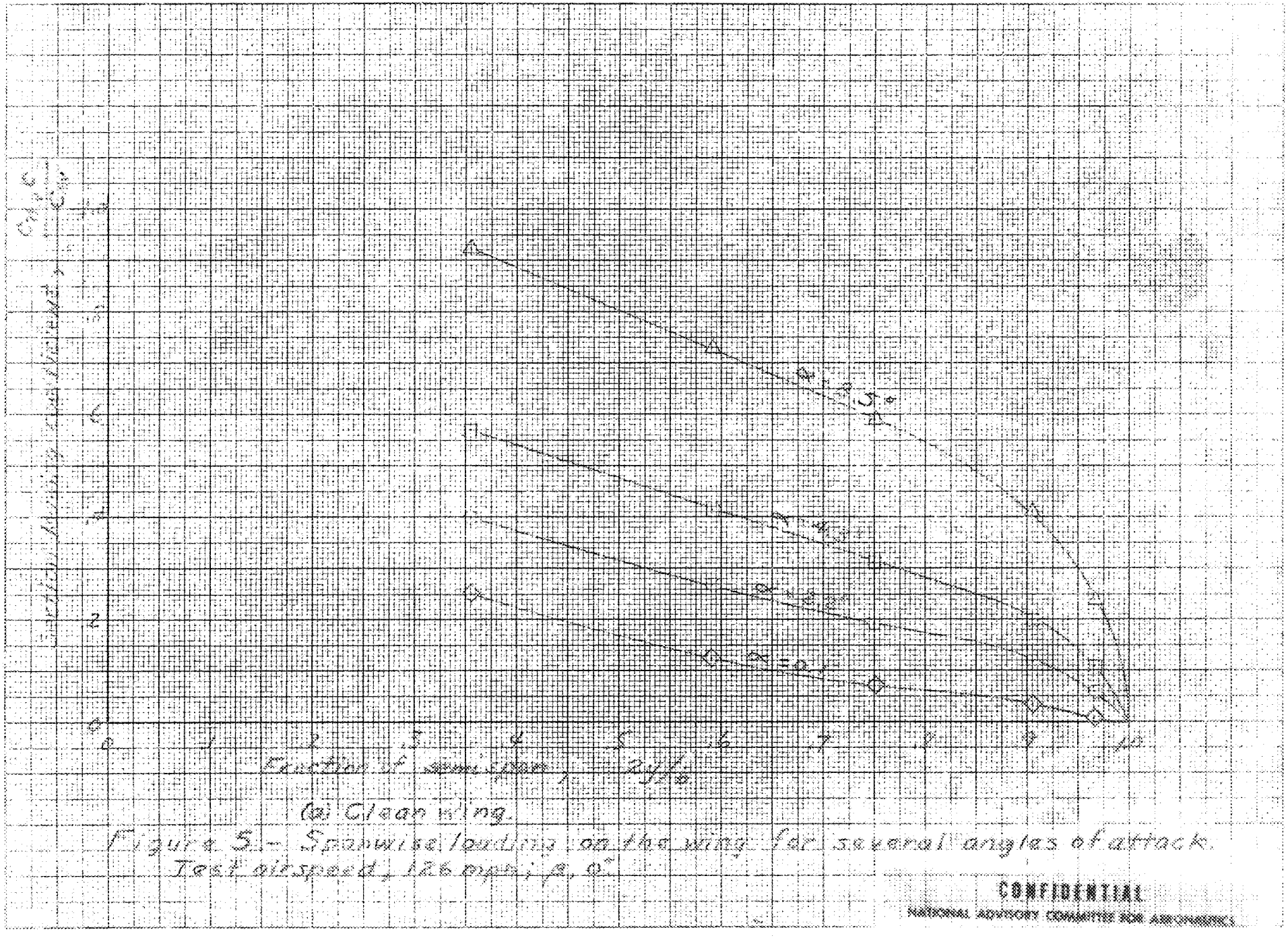

(a) Clean wing.

Figure 5.- Spanwise loading on the wing for several angles of attack. Test airspeed, 126 mph; q, q.

(b) Tip tank on.

Figure 5 - Continued

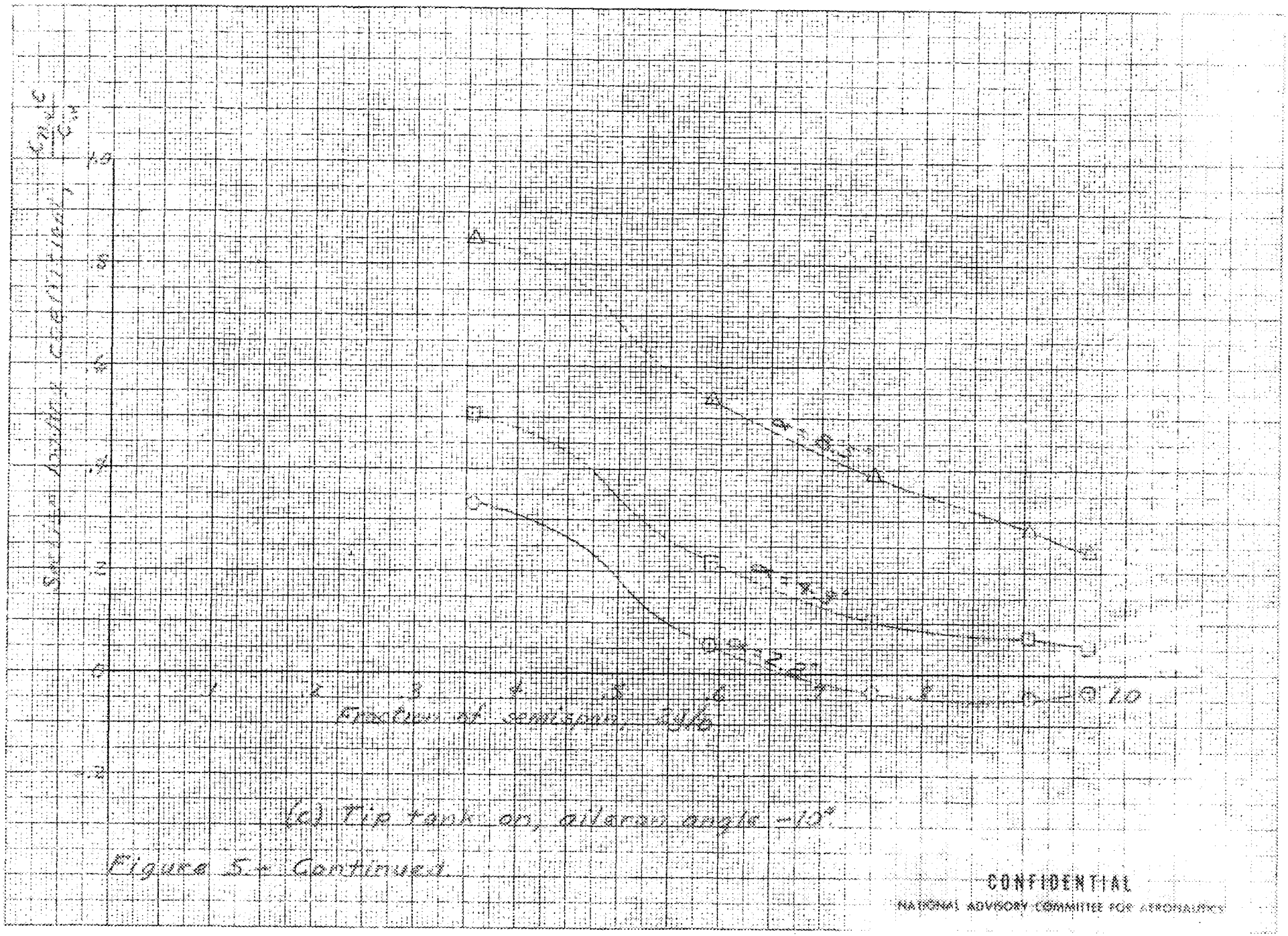

Figure 5.- Continued.

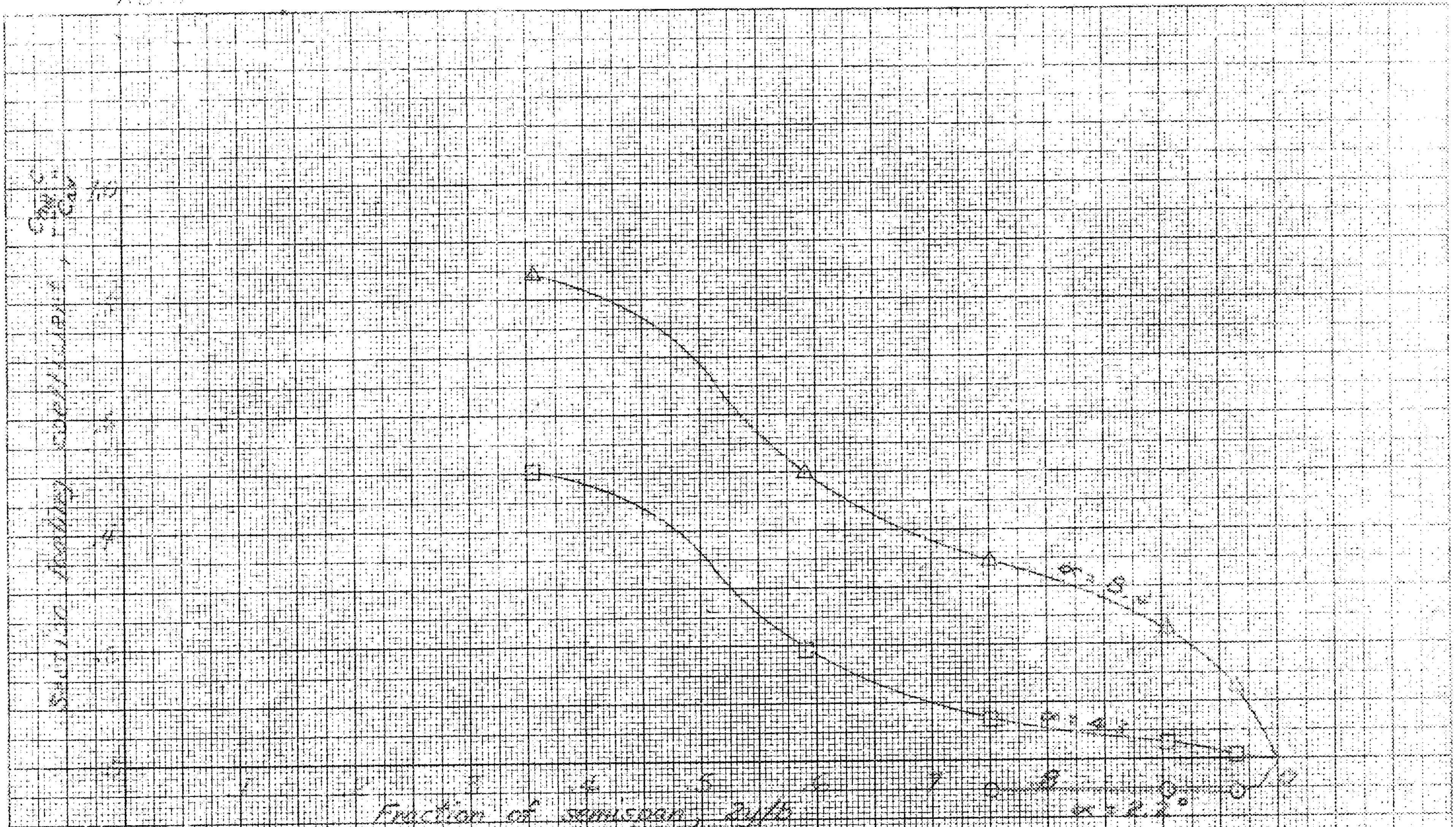

(d) Aileron angle -10°.

Figure 5.- Continued.

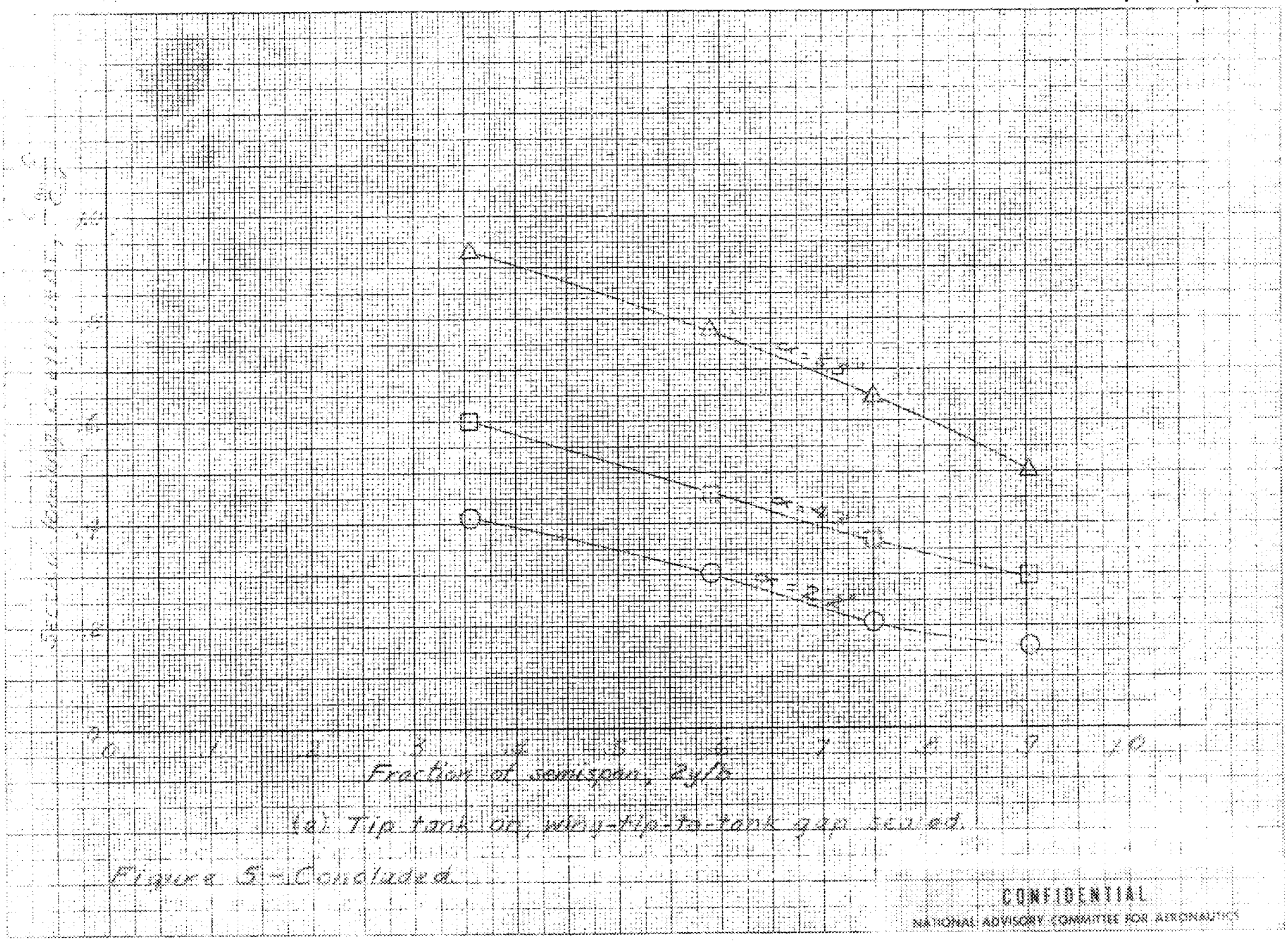

(a) Tip tank on wing-tip-to-tank gap sealed.

Figure 5.- Concluded.

(a) Clean wing.

Figure 6.- Effect of sideslip on the spanwise loading of the wing at several angles of attack. Test airspeed, 125 mph.

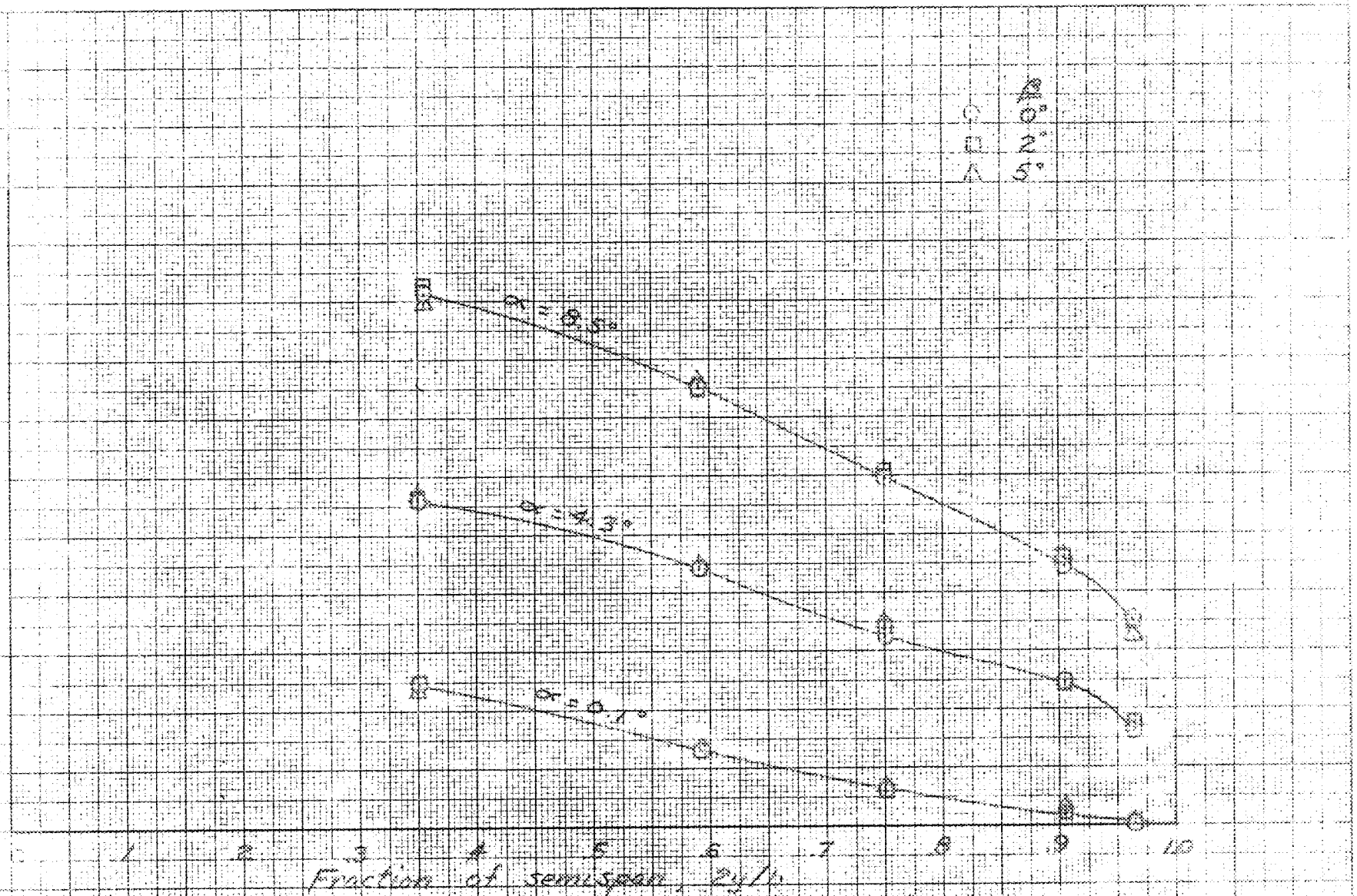

(d) Tip tank on.

Figure 6.- Continued.

(c) Tip tank on, dihedral angle -10°.

Figure 4.- Concluded.

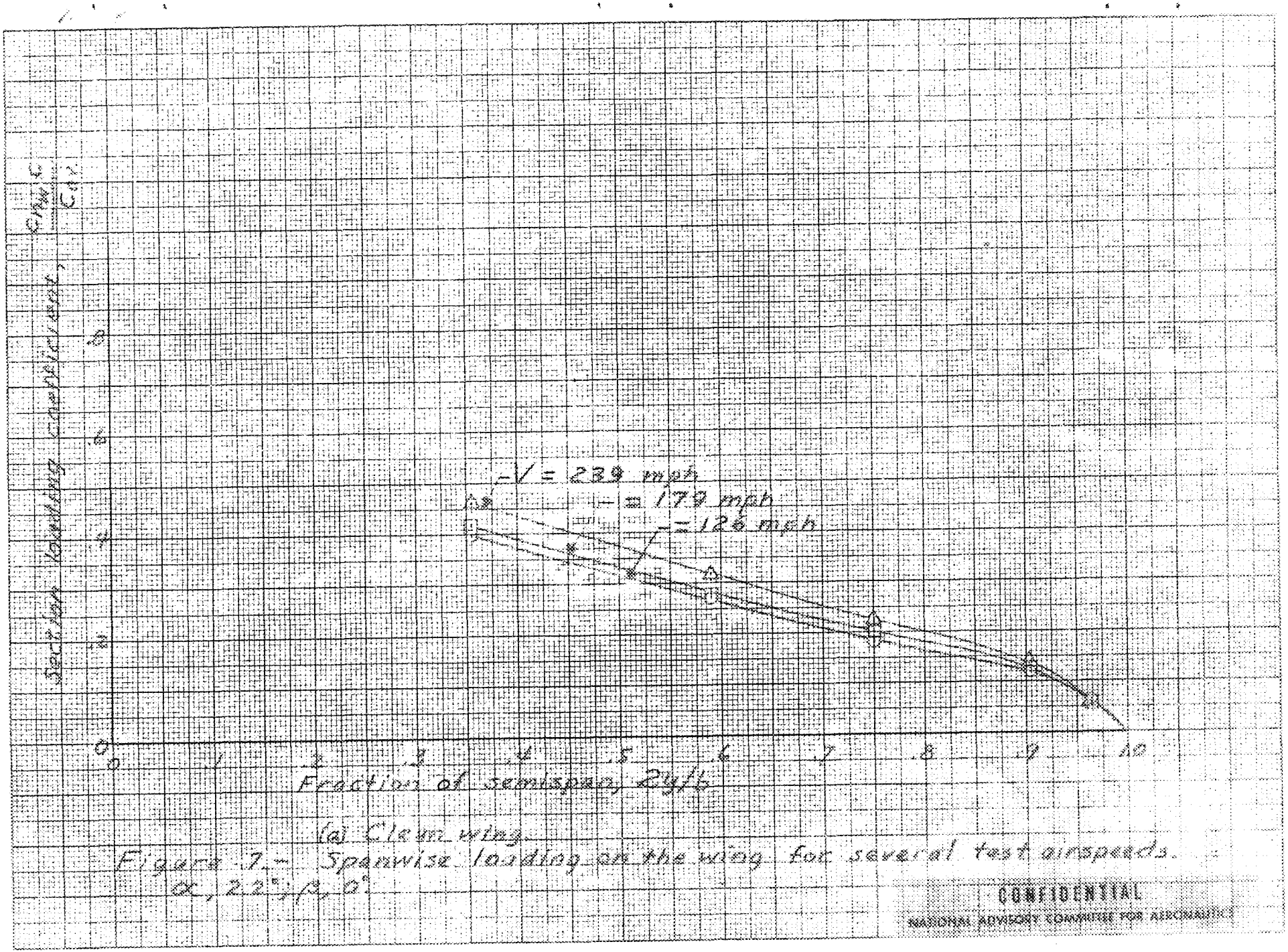

(a) Clean wing.

Figure 7.- Spanwise loading on the wing for several test airspeeds. α, 2.2°; β, 0°.

V = 233 mph
V = 179 mph
V = 126 mph
CONFIDENTIAL
NATIONAL ADVISORY COMMITTEE FOR AERONAUTICS

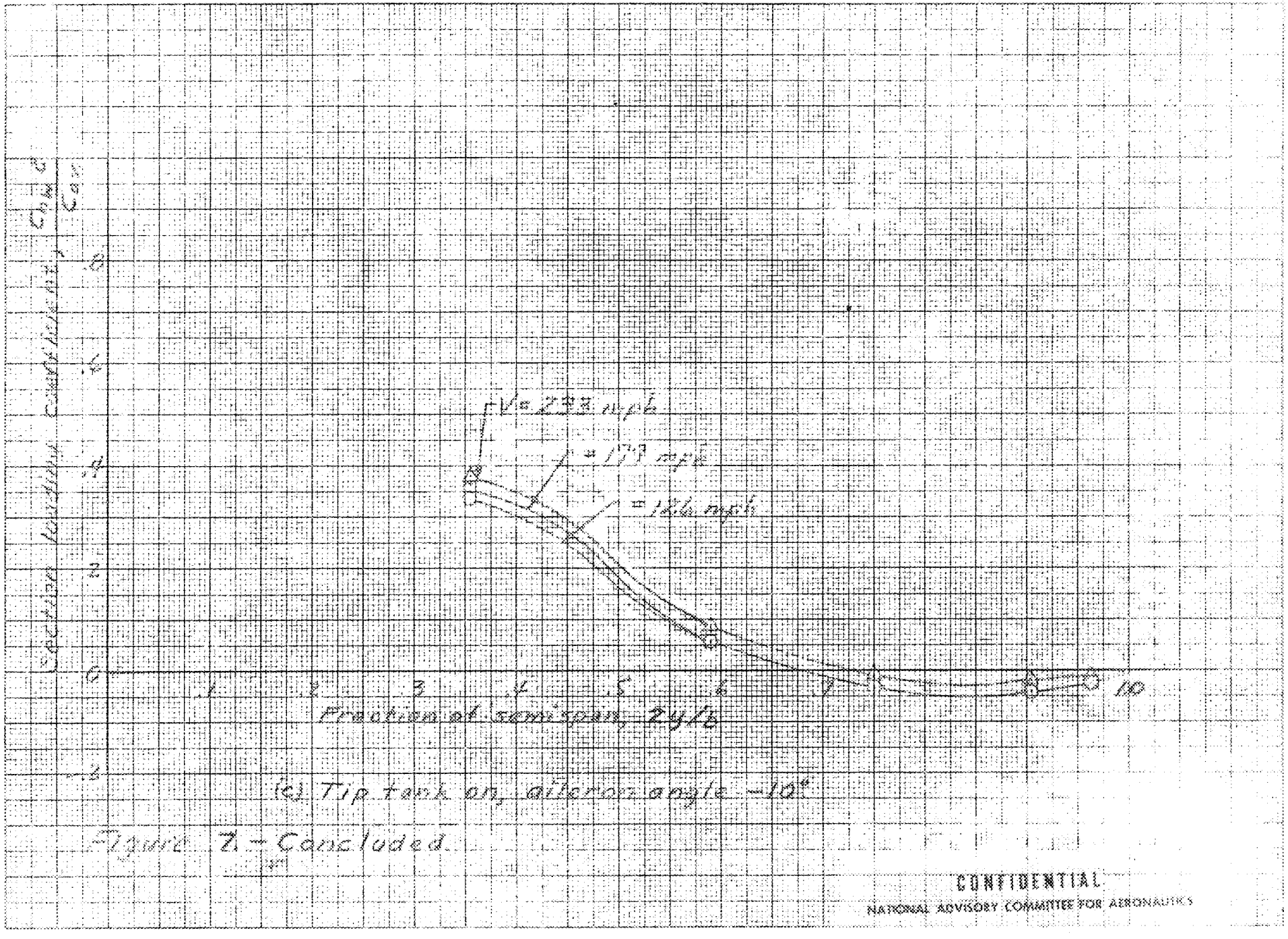

Figure 21.- Concluded.

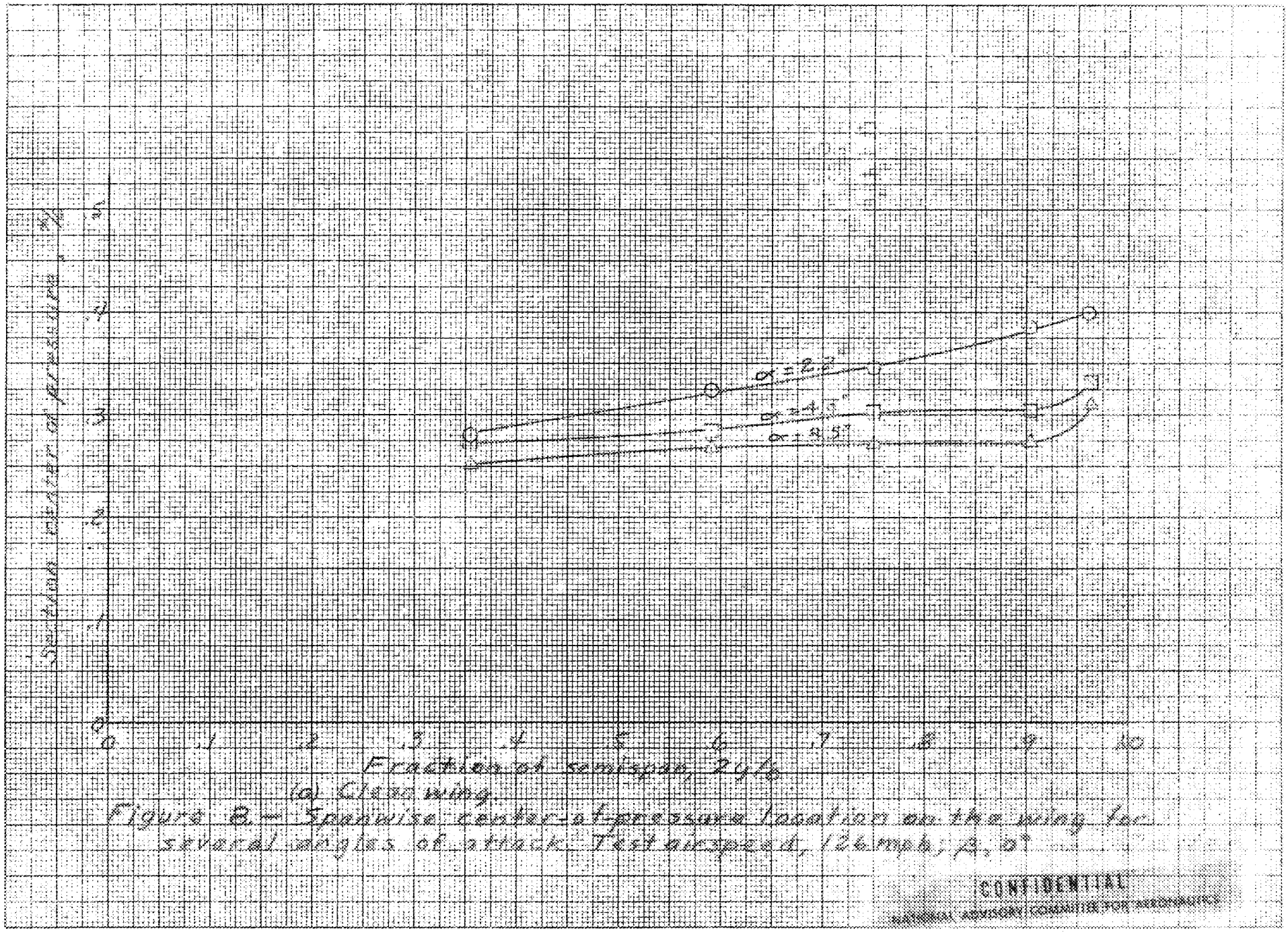

(a) Clean wing.

Figure 8.— Spanwise center-of-pressure location on the wing for several angles of attack. Test airspeed, 126 mph; β, 0°.

Figure 8.- Continued.

(c) Tip have an airfoil angle = 10°

Figure 8 - Concluded

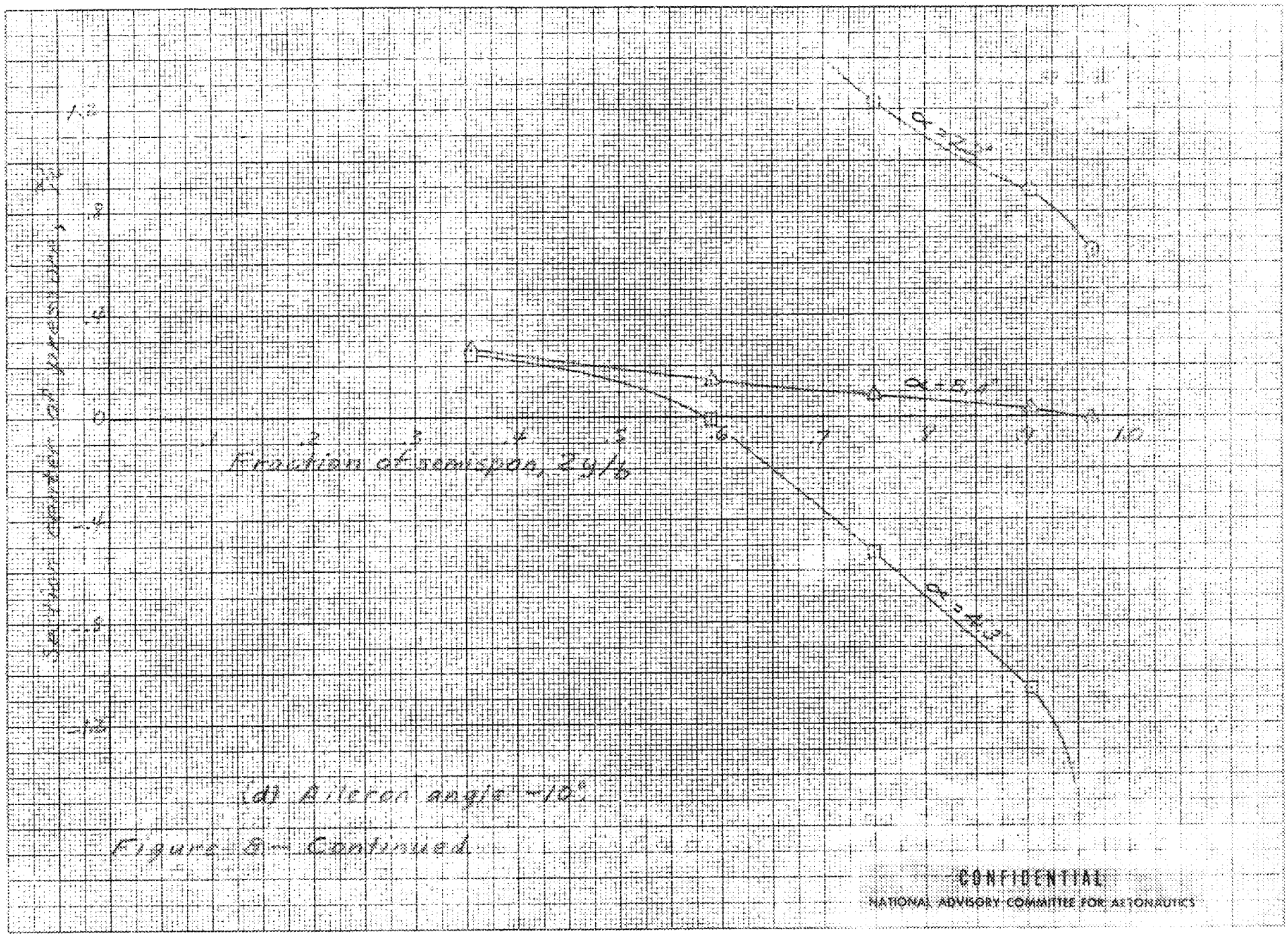

(d) Aileron angle $-10°$

Figure 8.- Continued

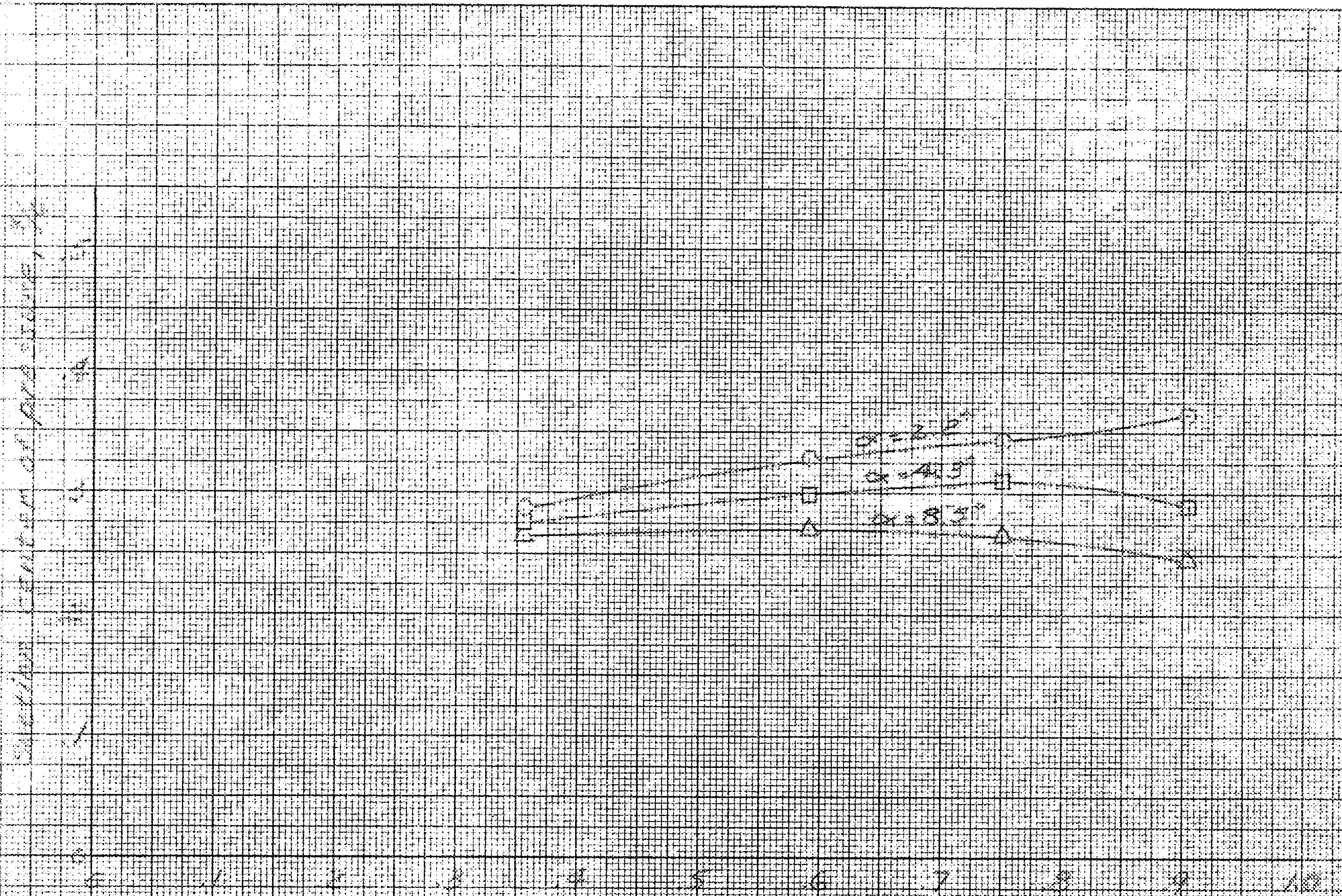

(c) Tip tank on, wing-tip-to-tank gap sealed.

Figure 8.- Concluded.

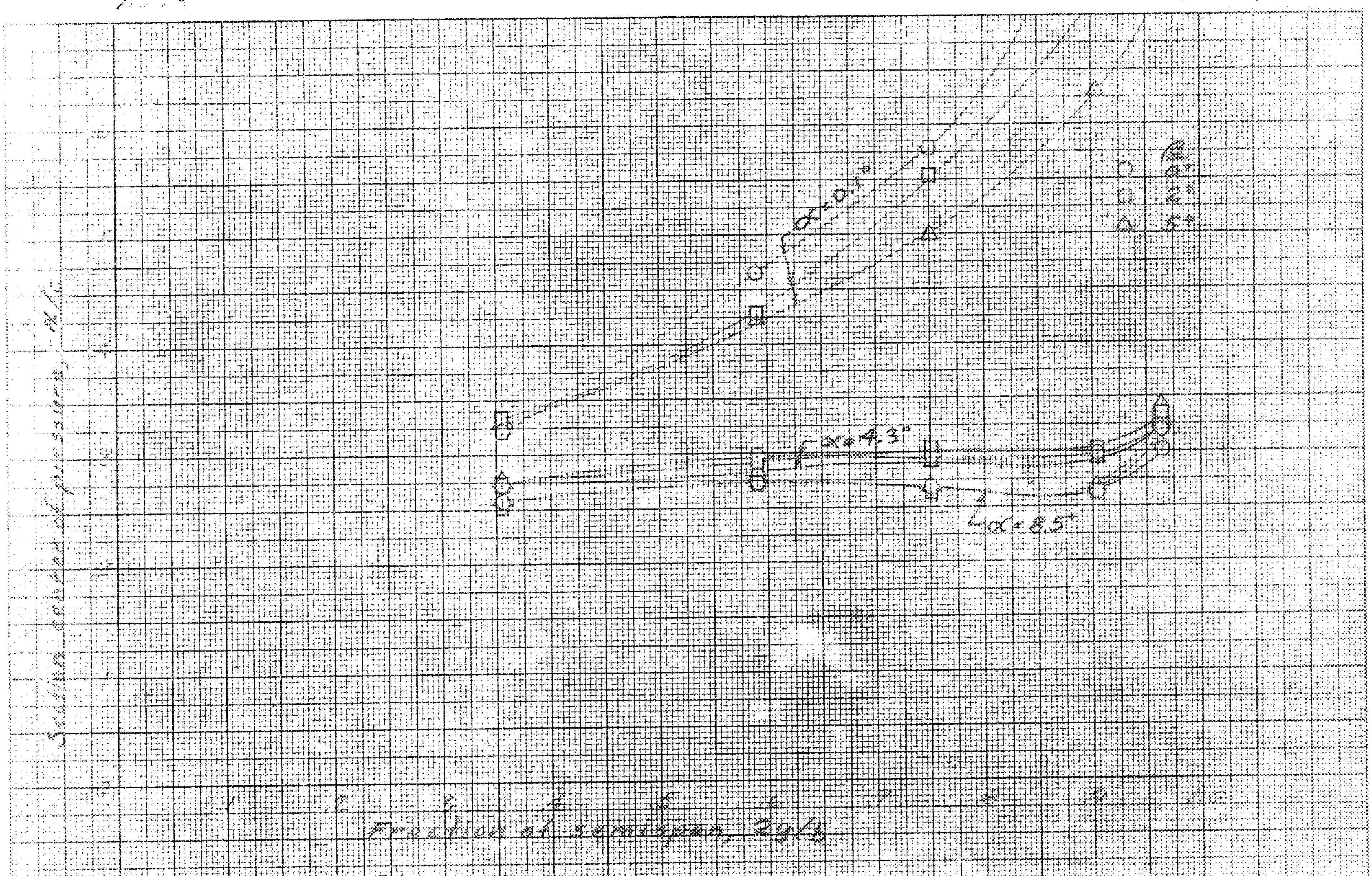

(a) Clean wing.

Figure 9.- Effect of sideslip on the spanwise center-of-pressure location on the wing at several angles of attack. Test airspeed, 126 mph.

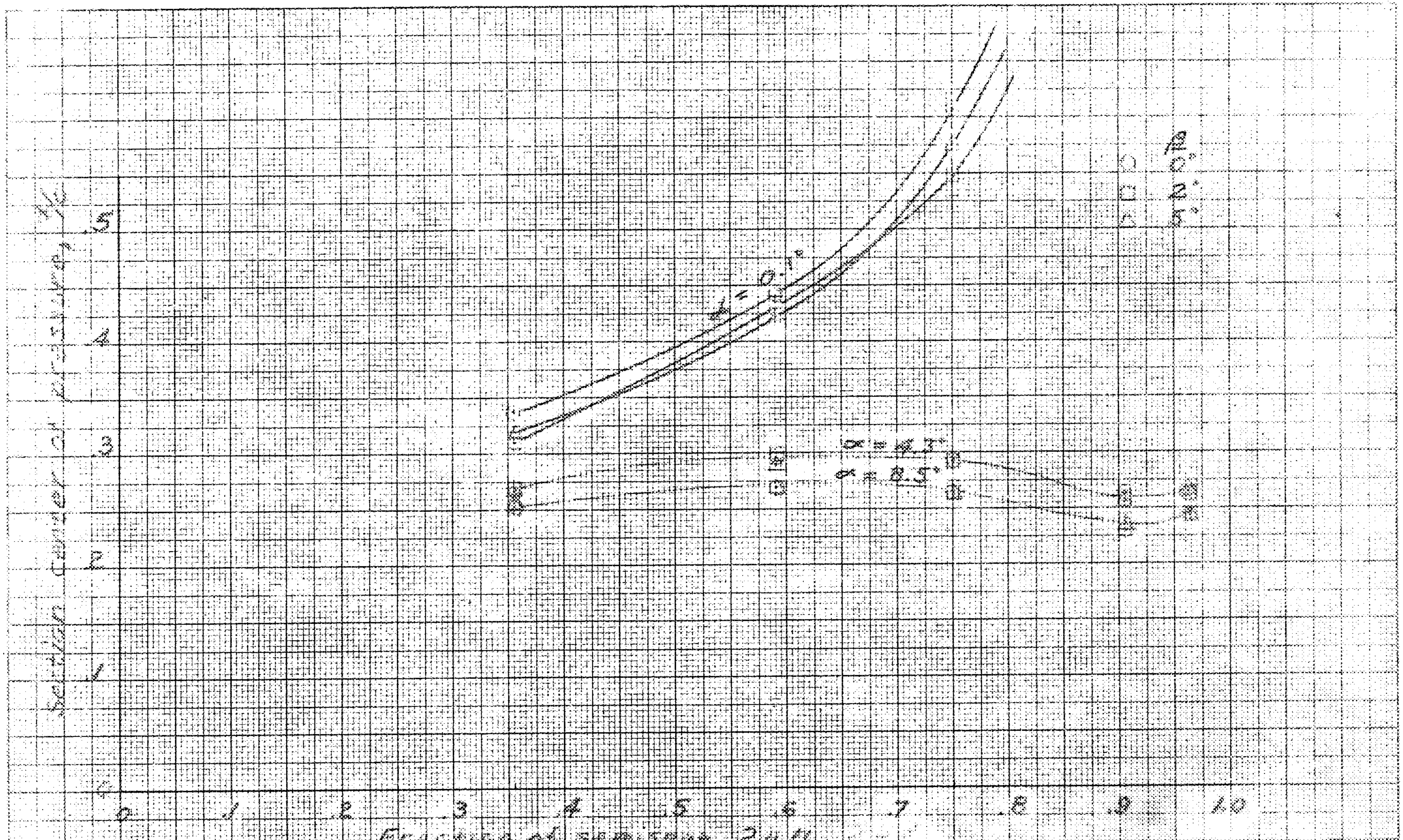

(b) Tip tank on.

Figure 9.- Continued.

Section center of pressure
(b) section of semispan, $2y/b$
(c) Top row, aileron angle $-10°$
Bottom row, aileron neutral
$\alpha = 8.1°$
$\alpha = 6.5°$
$\alpha = 4.3°$
CONFIDENTIAL
NATIONAL ADVISORY COMMITTEE FOR AERONAUTICS

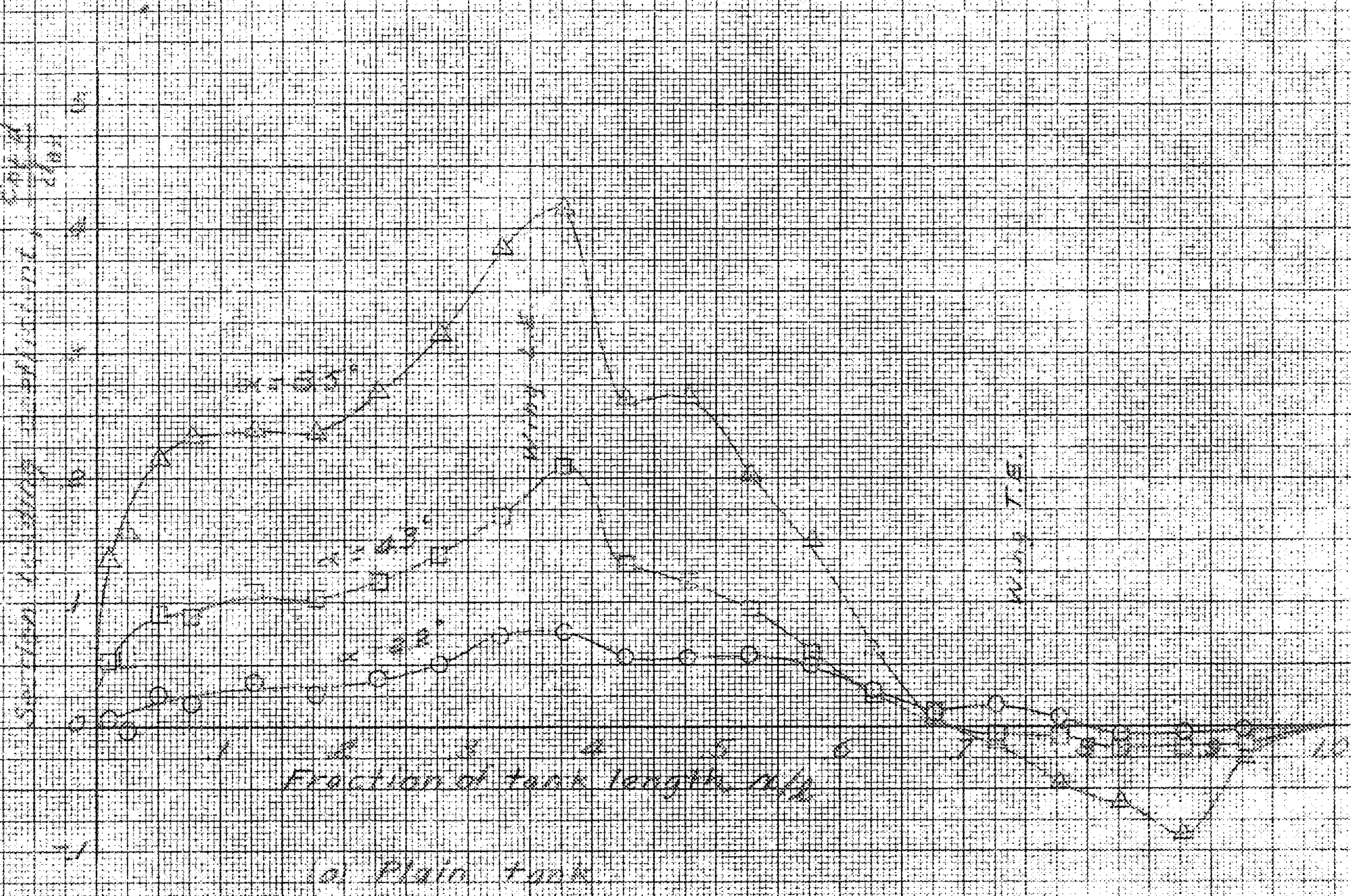

(a) Plain tank.

Figure 10. – Tank load distribution for several angles of attack. Test airspeed, 126 mph; β, 0°.

(b) Aileron angle −10°.

Figure 10.- Continued.

(c) Wing-to-tank gap sealed.

Figure 10.- Concluded.

Figure 11.- Wing load distributions for assumed test airspeeds. α, 2.2°; β, 0°.

(b) Aileron angle, $-10°$

Figure 11.- Concluded

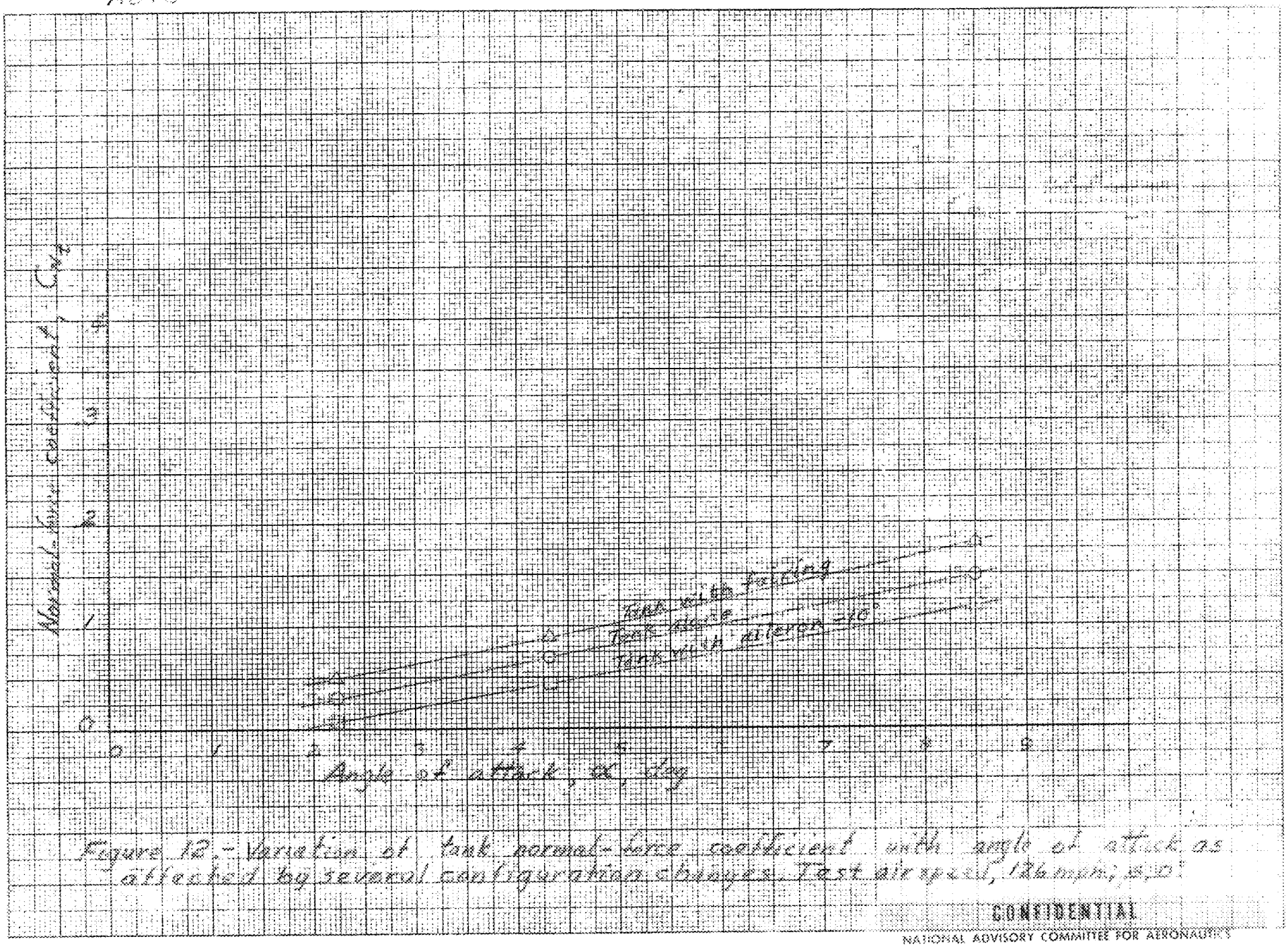

Figure 12.- Variation of tank normal-force coefficient with angle of attack as affected by several configuration changes. Test airspeed, 126 m.p.h.; $\alpha_t = 0°$.

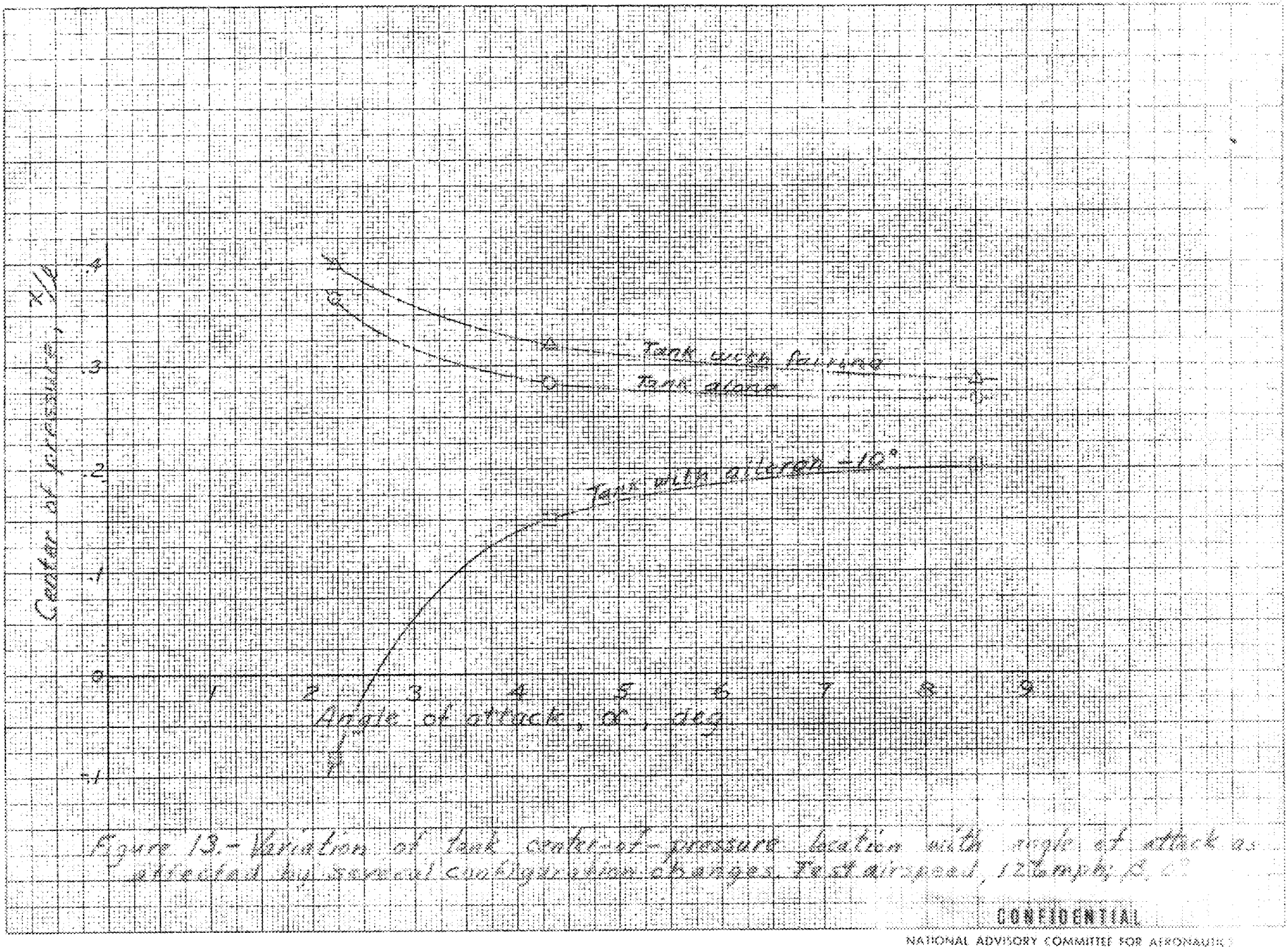

Figure 13.- Variation of tank center-of-pressure location with angle of attack as affected by various aerodynamic changes. Test airspeed, 125 mph; R, 2.0×10^6.

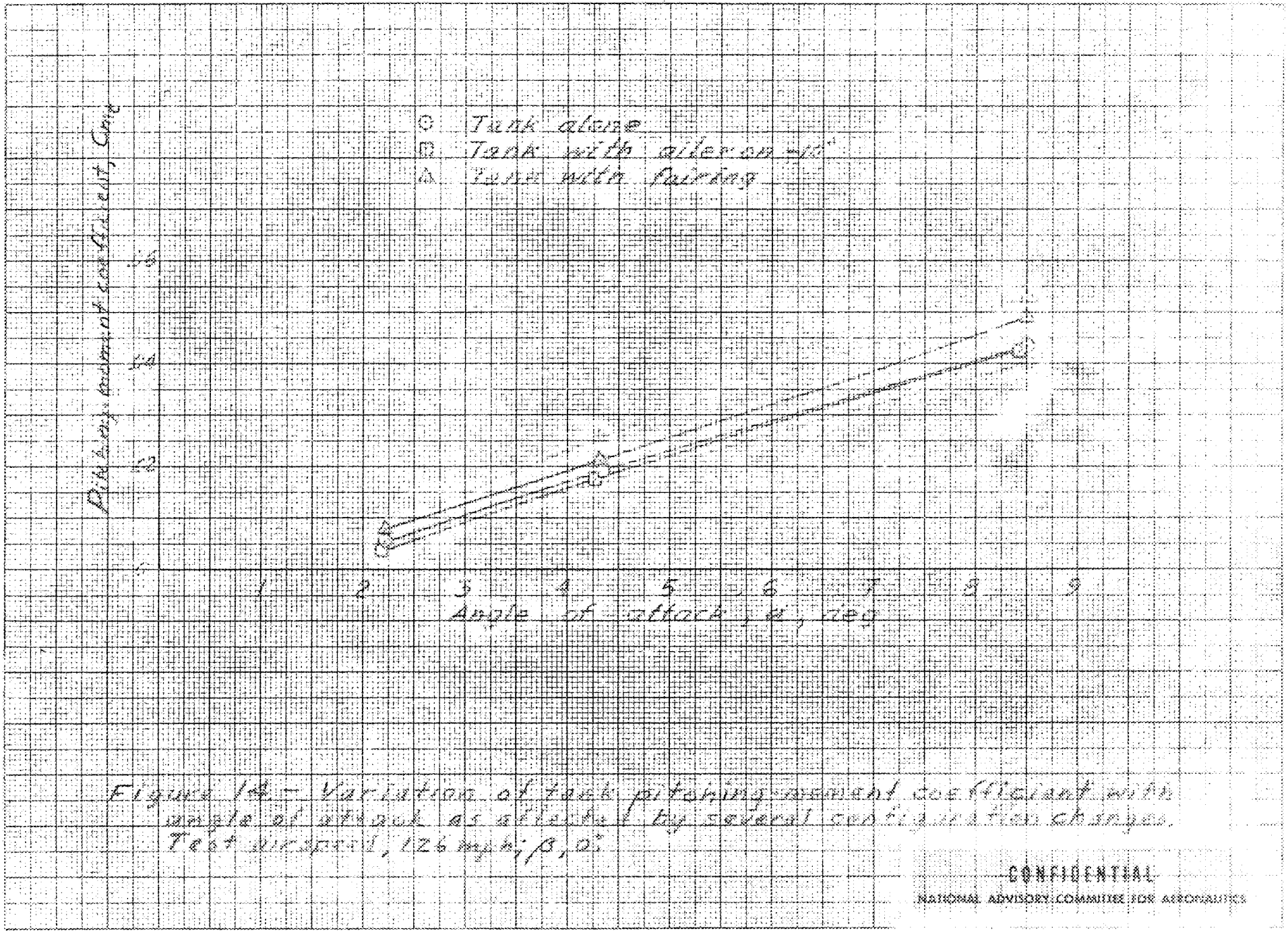

Figure 18.- Variation of tank pitching-moment coefficient with angle of attack as affected by several configuration changes. Test airspeed, 126 mph; β, 0°.

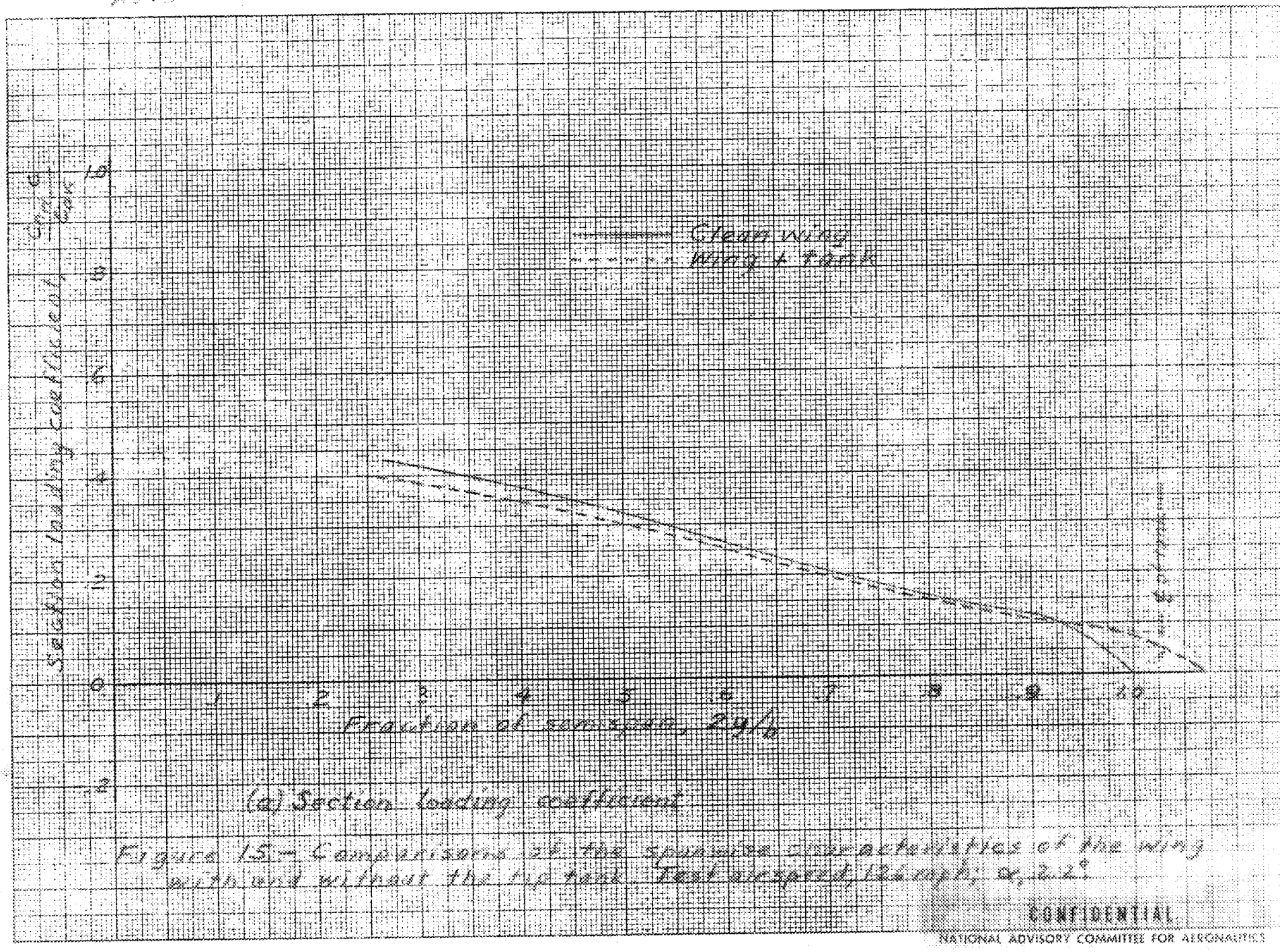

Figure 15.— Comparisons of the spanwise lift characteristics of the wing with and without the fuselage. Free-stream Mach number, M_0, 2.2; α_0, 2.2°.

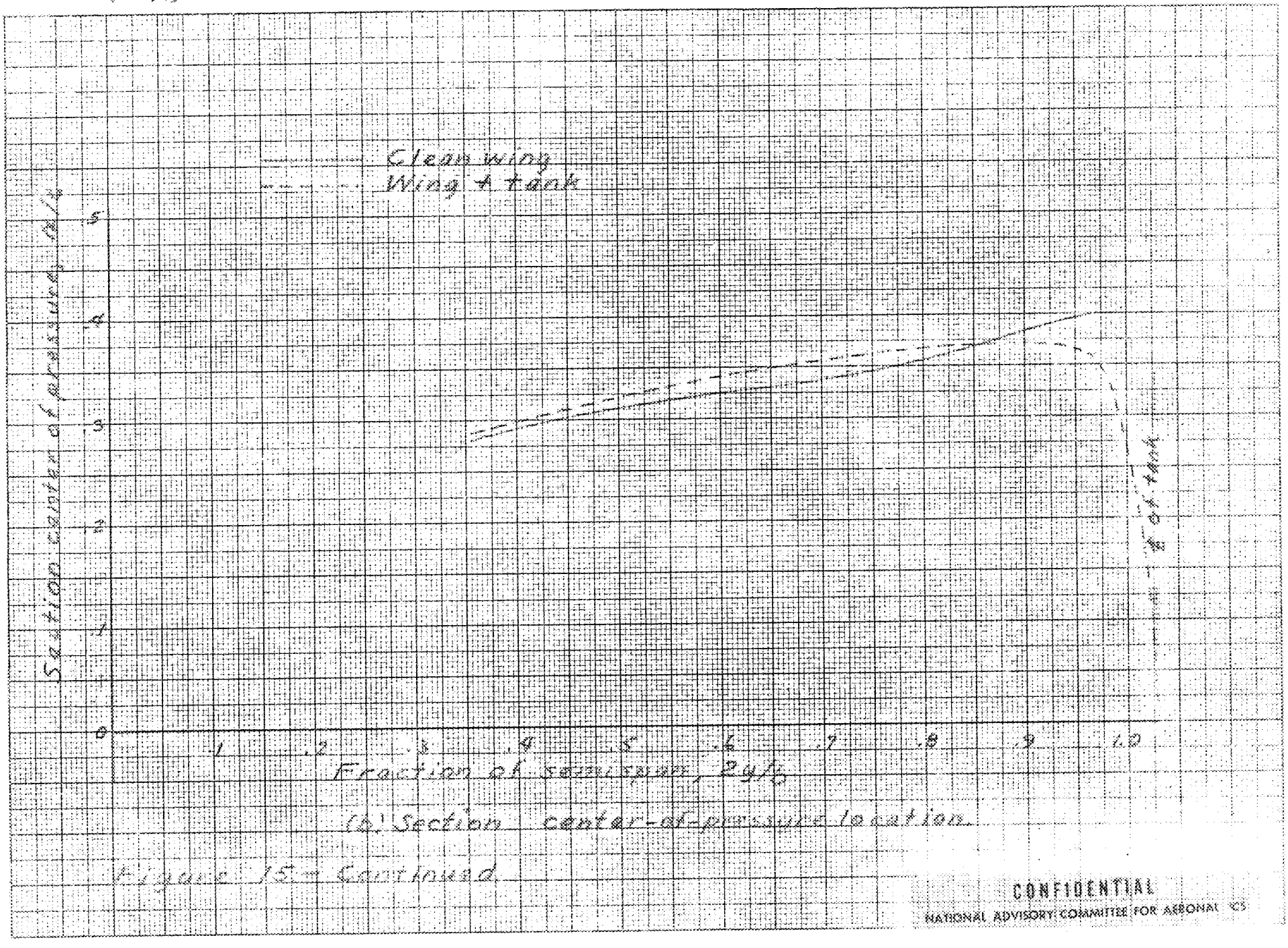

(b) Section center-of-pressure location.

Figure 15 - Continued.

(c) Section pitching-moment coefficient.

Figure 15 — Continued

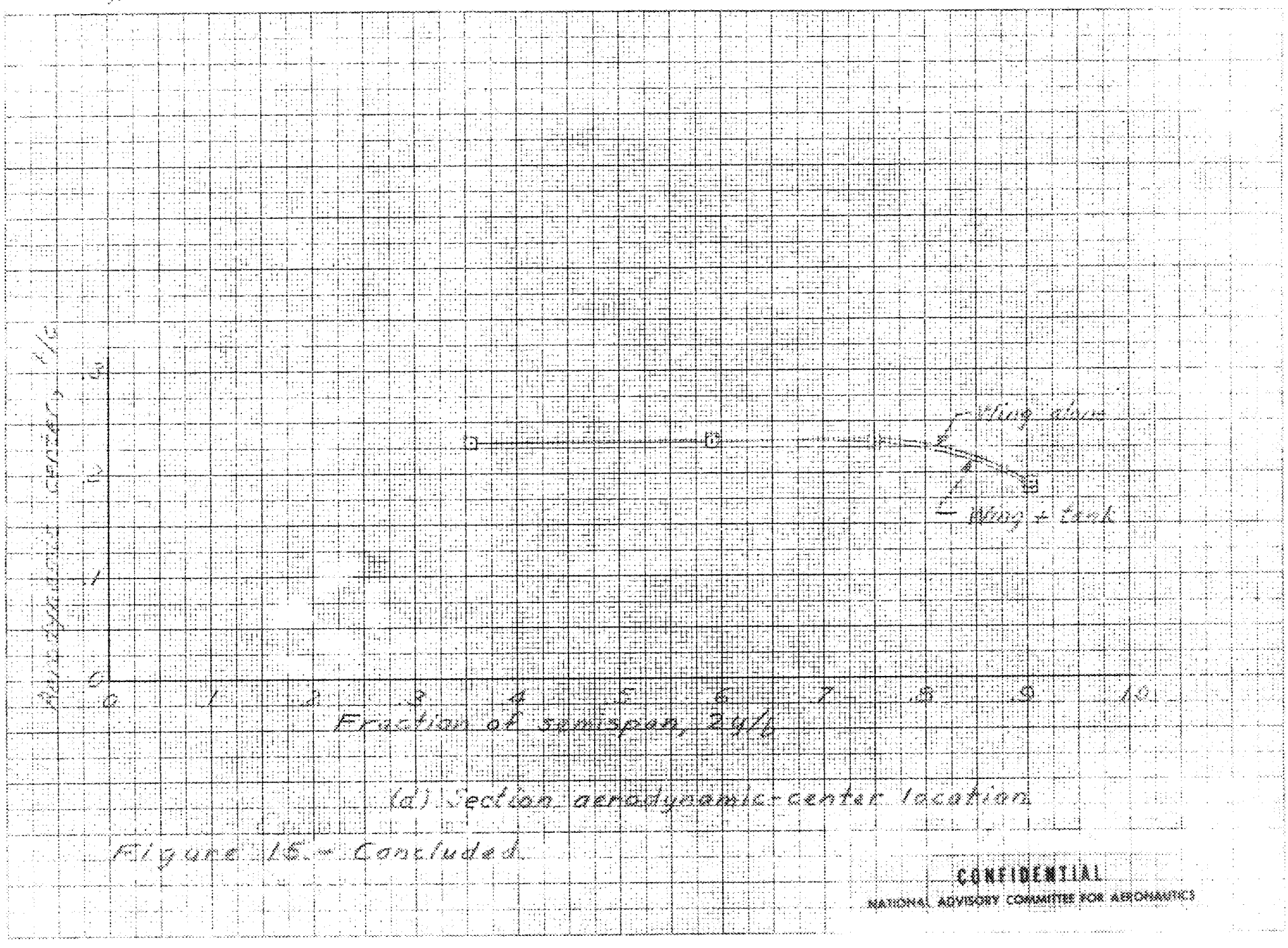

(a) Section aerodynamic-center location.

Figure 16.- Concluded.

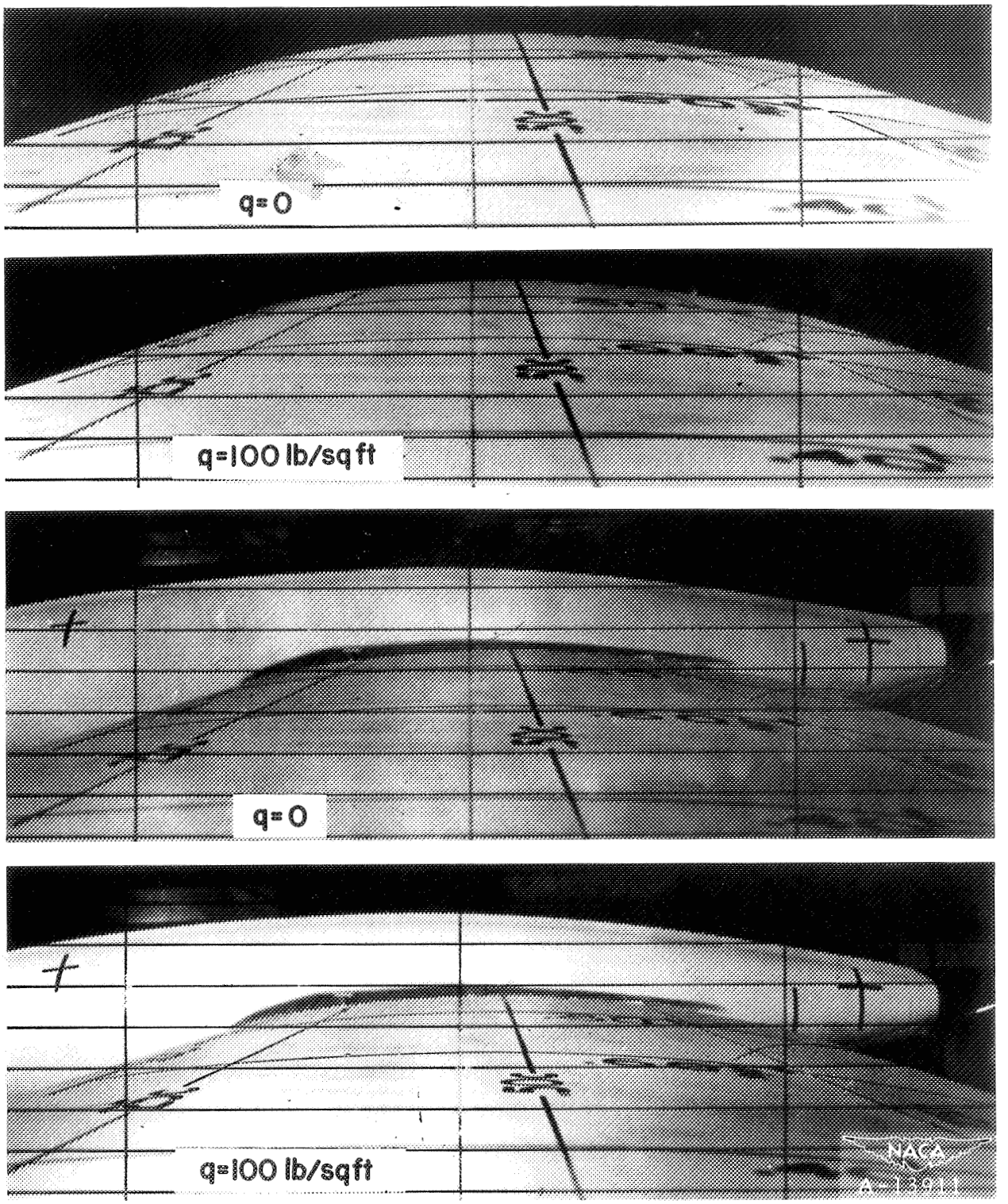

(a) α, 2.2°.

Figure 16.- Sample aeroelastic twist measurement photographs of the wing with and without the tip tank. β, 0°.

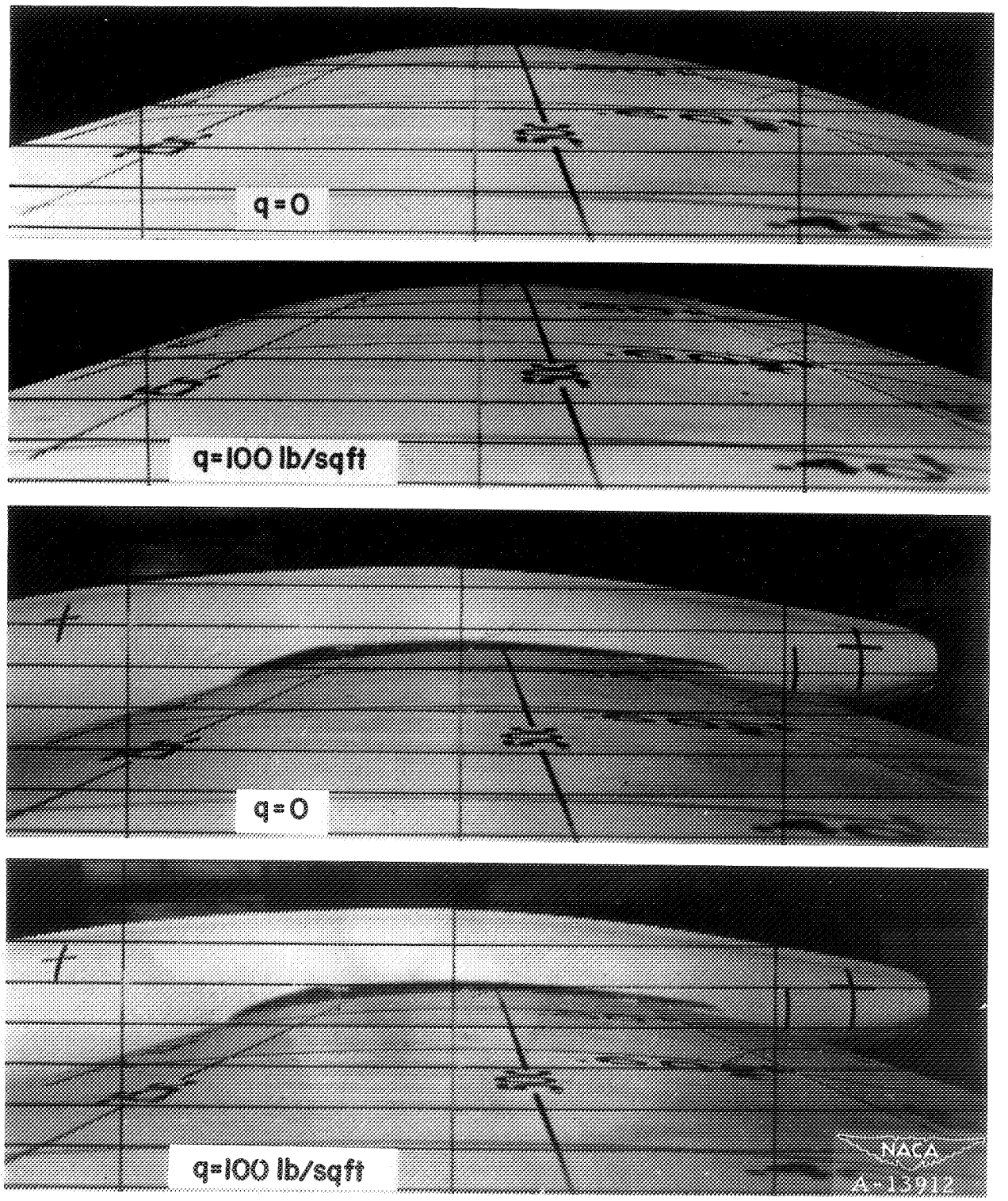

(b) α, 4.3°.

Figure 16.- Continued.

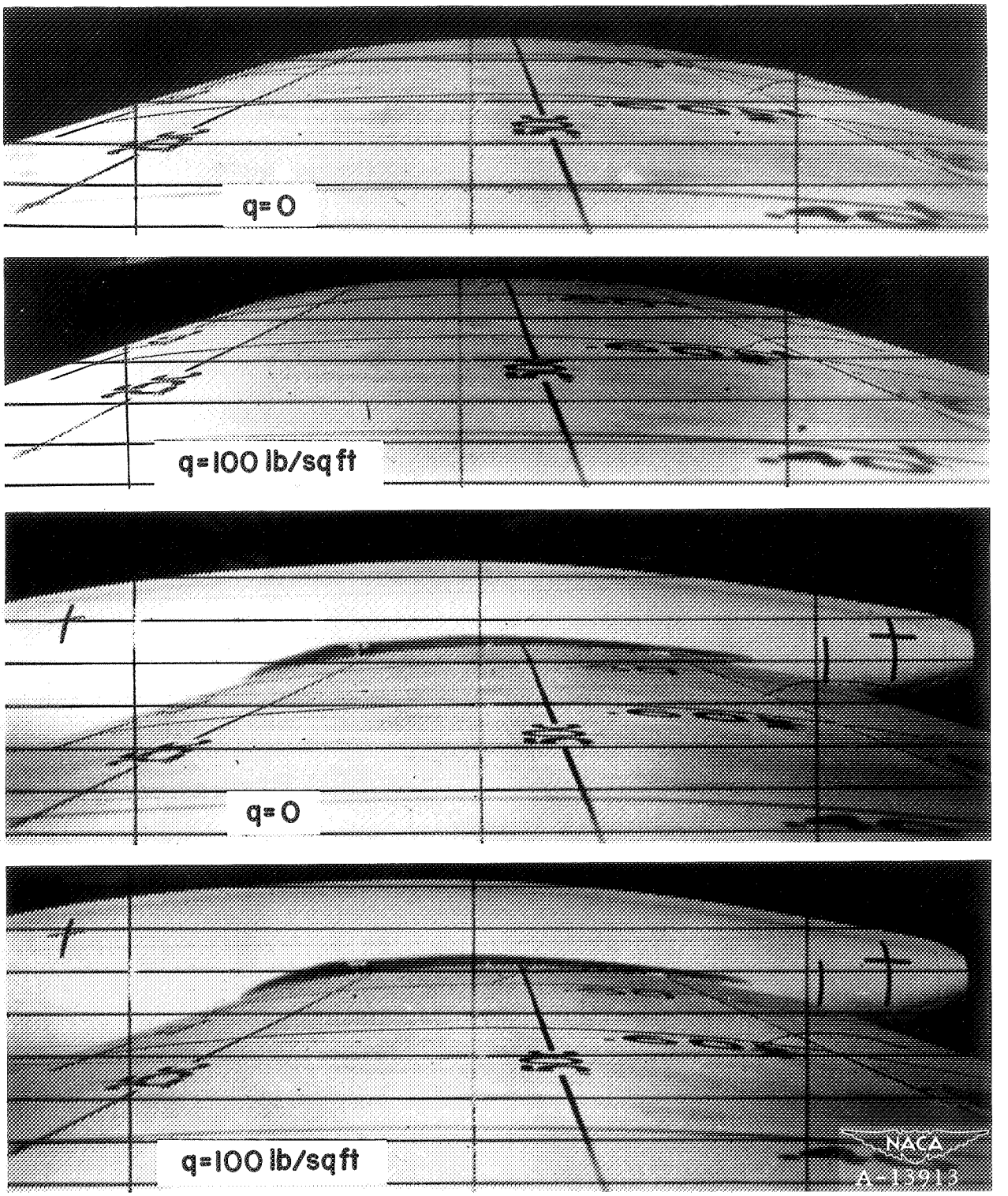

(c) α, 8.5°.

Figure 16.- Concluded.

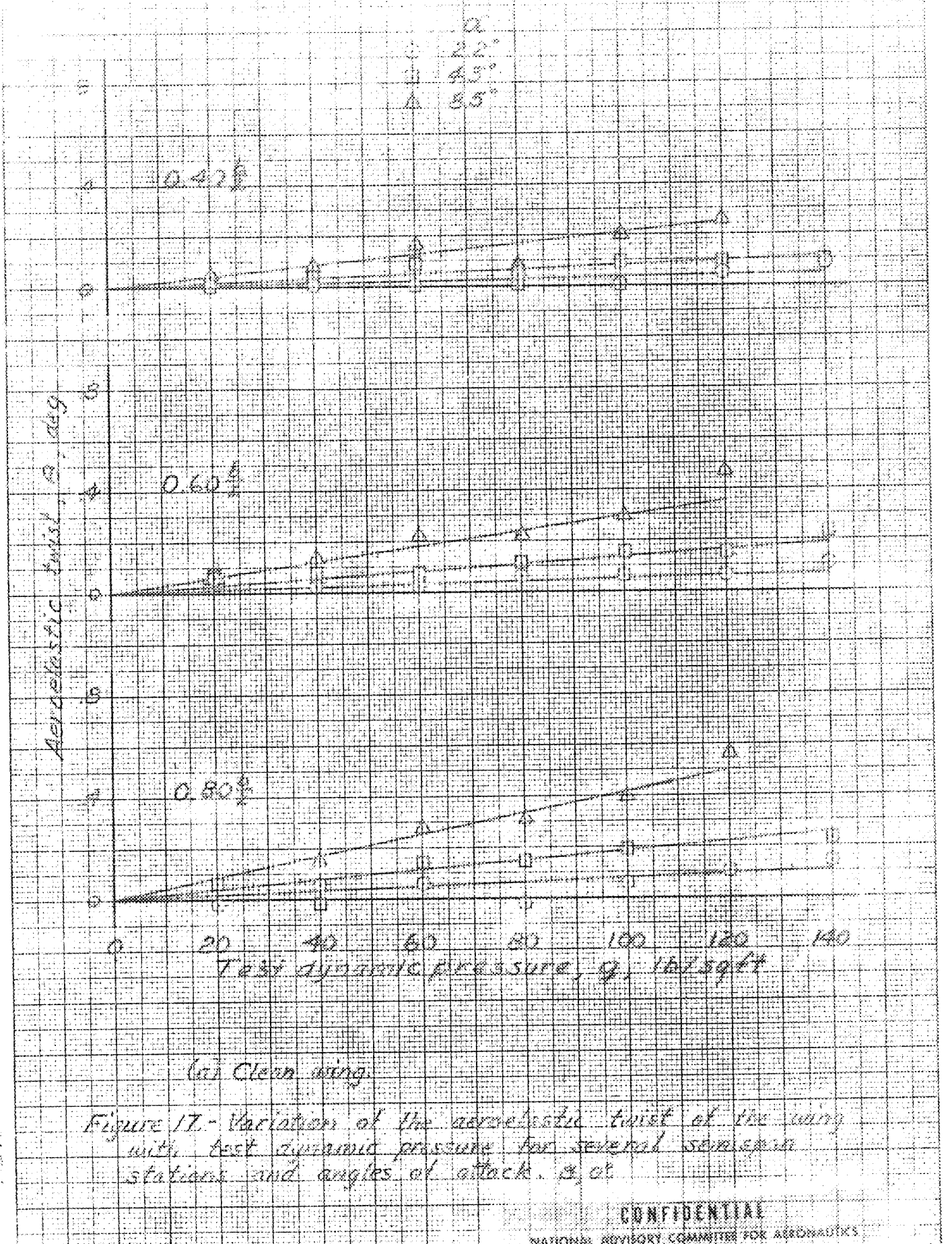

(a) Clean wing.

Figure 17.- Variation of the aeroelastic twist of the wing with test dynamic pressure for several semispan stations and angles of attack, α, at

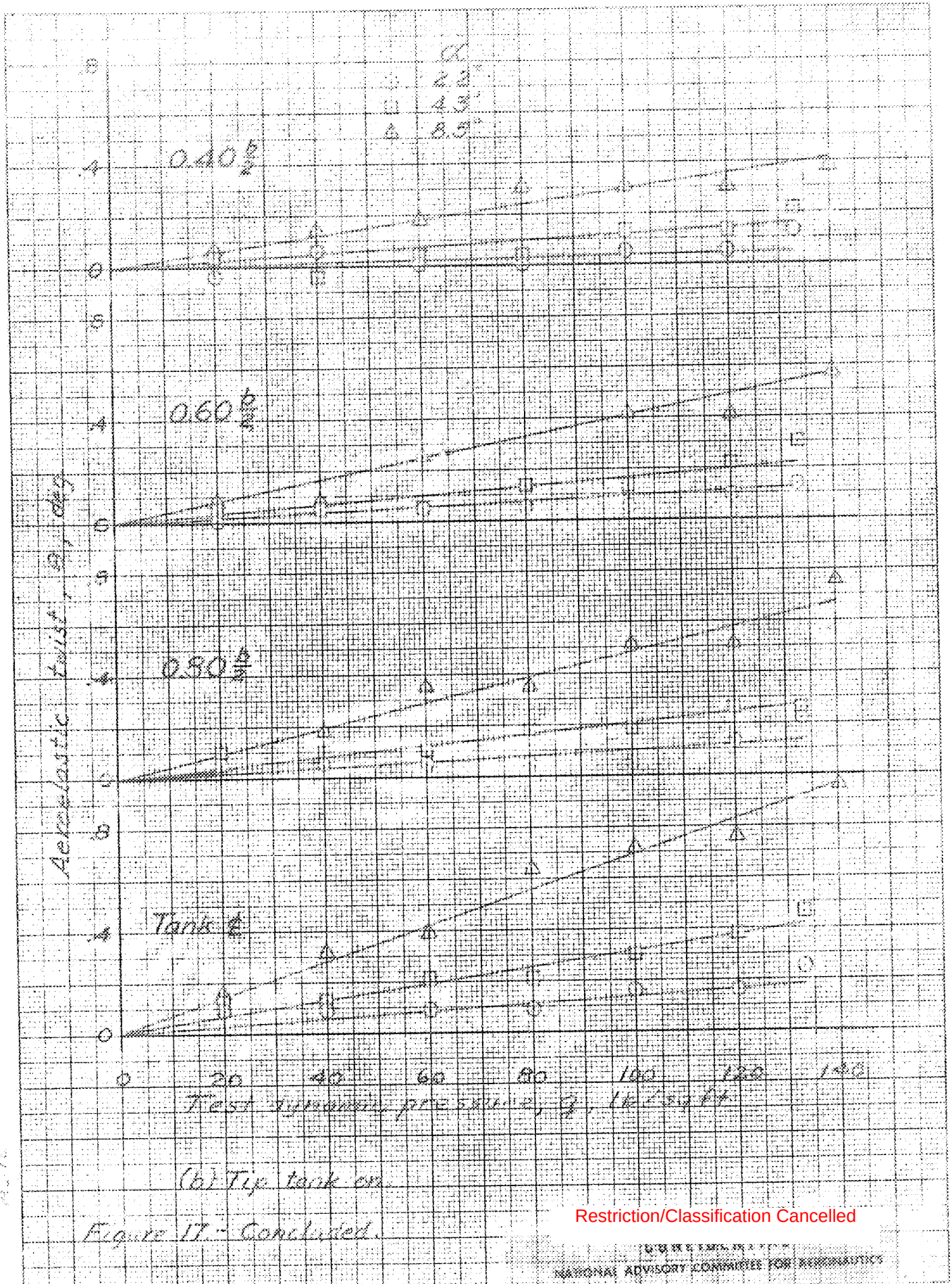

(b) Tip tank on.

Figure 17.- Concluded.